ABSTRACT

DENNING, STEFANIE CLAIRE. Dual Strategy for Characterizing foxq1b. (Under the direction of Dr. Antonio Planchart).

FOXQ1 is a transcription factor that regulates gastric acid secretion, hair follicle formation, and craniofacial patterning in mammalian development. FOXQ1 is overexpressed in certain cancer cells and is associated with cancer progression and metastasis. Since much is still unknown about *FOXQ1*, we chose to study the function of the zebrafish ortholog, *foxq1b*. Zebrafish are genetically similar to humans, making them a useful *in vivo* model for human studies. Zebrafish are also advantageous because their embryos are transparent and development is external. These qualities allow for genetic manipulations and phenotypic observations to be performed at early stages of development. Preliminary data has shown that, like mammalian *FOXQ1*, zebrafish *foxq1b* is important for proper craniofacial formation, and when knocked down results in severe jaw abnormalities. Through next generation sequencing (NGS) studies, *foxq1b* has been shown to regulate numerous genes that contribute to proper embryonic development as well as the progression of cancer. In order to gain a better understanding of FOXQ1's role in development and cancer, a transgenic zebrafish that contains an allele of *foxq1b* tagged with the myc epitope at the C-terminus was created through molecular cloning and microinjections into one-cell stage zebrafish embryos. Chromatin immunoprecipitation using an anti-myc antibody may be performed using this transgenic zebrafish to locate where in the genome foxq1b binds. This method will be used to uncover the regulatory landscape controlled by foxq1b, thus providing possible insights into the role of the human ortholog in development and disease. To compliment the knowledge we will gain through the use of the myc-tag *foxq1b* transgenic, we utilized CRISPR-Cas9

technology to generate null alleles of the *foxq1b* gene, in order to better understand its role in vertebrate development. The results of our research will provide the scientific community with important tools needed for further studies on the involvement and importance of *FOXQ1*throughout both embryonic development and cancer formation.

Dual Strategy for Characterizing foxq1b

by
Stefanie Claire Denning

A thesis submitted to the Graduate Faculty of
North Carolina State University
in partial fulfillment of the
requirements for the degree of
Master of Science

Zoology

Raleigh, North Carolina

2015

APPROVED BY:

_____	_____
Dr. Antonio Planchart Co-Chair of Advisory Committee	Dr. Nanette Nascone-Yoder Co-Chair of Advisory Committee

_____
Dr. Beth Hawkins

DEDICATION

I dedicate this work to my family, especially my parents Deb and Steve Denning. You have been so patient and helpful throughout my educational experience. Thank you for always supporting and encouraging me to further my education in science. I love you guys.

BIOGRAPHY

Stefanie Claire Denning was born in Geneva, New York on October 1, 1991. She moved to Raleigh, North Carolina when she was 5 years old. She graduated from Cardinal Gibbons High School and attended North Carolina State University for her undergraduate degree in Biology with a concentration in Human Biology. During her senior year, she worked in a Plant Pathology lab at NC State, where she gained an interest in research. She decided to apply for graduate school to further pursue her interest in research within the biology field. She graduated with her Bachelor's degree in May 2013 with *Summa Cum Laude*, and in August 2013 began her Master's degree in Zoology at North Carolina State University under Dr. Antonio Planchart.

ACKNOWLEDGMENTS

I would like to thank my advisor Antonio Planchart for giving me the opportunity to work on this research project. Also for all of his support and guidance along the way. I have learned so much from him over the past two years.

I am very grateful for my committee members for all of their advice and encouragement: Dr. Nanette Nascone-Yoder and Dr. Beth Hawkins. I sincerely appreciate all of Carolyn Mattingly, David Chris Cole, and Norma Escalante's help in the lab. My project would not have gone as smoothly without them. Special thanks to Elizabeth Cook and Lindsey St. Mary for being very helpful and encouraging in the lab, and to all of our good times.

I would like to thank the Biology Department for providing my funding through my teaching assistantship. Lastly, I am thankful for my family, my boyfriend Andrew Howell, and all my friends who have been very supportive throughout this process.

TABLE OF CONTENTS

LIST OF TABLES

LIST OF FIGURES

I. LITERATURE REVIEW

Introduction

The prototype forkhead box gene (*fkh)* was discovered in a mutagenesis screen of *Drosophila melanogaster* homeotic transformants (Jürgens and Weigel 1988). Forkhead box (Fox) genes are a family of transcription factors whose name derives from the phenotype: mutations in *Drosophila fkh* cause the appearance of a two-spiked head structure, resembling a fork (Carlsson and Mahlapuu 2002). At present, there are 19 subfamilies, FoxA through FoxS, in mammals; within each subfamily, there can be multiple genes, each of which is identified by a number (Table 1 and Jonsson and Peng 2005). Fox genes contain an 80 to 110 amino acid DNA binding domain called the “forkhead box” or "winged helix" domain, the latter named from its X-ray crystallography structure that is comprised of three α–helices linked by two β–loops (Carlsson and Mahlapuu 2002). This domain allows them to bind to and regulate certain genes contributing to the growth and formation of an organism’s body structure (Wotton and Shimeld 2011). Fox proteins identified in mice and humans are found to play an important role in not only development but also metabolism and immunoregulation. Although Fox genes are critical for many cellular functions, misregulation of these genes can contribute to aging and cancer (Jonsson and Peng 2005). Adequate regulation of Fox genes is essential for maintaining fundamental processes that are required for cell growth and survival.

Genome sequencing projects have concluded that Forkhead genes are only present in the animal and fungi kingdoms. *Saccharomyces* and *Schizosaccharomyces spp.* contain 4,

Caenorhabditis spp. contain 15, *Drosophila spp.* contain 20, and mammals contain over 40 Fox gene family members (Carlsson and Mahlapuu 2002, Hannenhalli and Kaestner 2009); therefore, the number of Fox genes an organism possesses appears to be directly proportional to the structural complexity of that organism.

Throughout evolution, many genome duplications have occurred resulting in a gain, loss, or change in genetic information (Crow and Wagner 2006). In the animal kingdom, vertebrates underwent two genome duplications prior to the divergence of fish and mammals. After the branching of the mammalian linage, a third genome duplication occurred in fish. Since zebrafish contain two paralogs for many mammalian genes, it is thought that this third genome duplication resulted in polyploidization, which is a multiplication of a whole chromosome (Postlethwait 1998). When paralogs are generated from a genome duplication, they may diverge: one paralog may acquire a new function (neofunctionalization); alternatively, the ancestral function may be split between the two paralogs (subfunctionalization); and lastly, one paralog may retain the original function subject to selection whereas the other may degenerate (Presgraves 2005). The Fox gene family has multiplied and acquired new members with distinct roles throughout evolution (Lynch and Conery 2000). Many of the Fox genes and their specific functions have been studied in various organisms, including zebrafish, and compared to their human orthologs.

One particular member of the vertebrate forkhead box transcription factor family, *FOXQ1*, is a 403 amino-acid protein whose winged helix amino acid sequence is identical between rats, mice, and humans indicating its evolutionary conservation in mammalian

species (Bieller 2001, Hong 2001). The zebrafish paralogs, *foxq1a* and *foxq1b*, are also structurally similar to mammalian *FOXQ1* (Planchart and Mattingly 2010). The role of *FOXQ1* in development and disease, as well as, how it is regulated and how it regulates gene expression will be discussed in the following sections.

Upstream Regulators of *FOXQ1*

FOXQ1 interacts with signaling pathways and gene families that are crucial for growth and development. Important pathways and genes that involve *FOXQ1* are: hedgehog and Wnt signaling pathways, transforming growth factor beta (TGFβ), Aryl hydrocarbon receptor (AhR), Homeobox (Hox) genes, and the retinoic acid pathway. The hedgehog signaling pathway and the Wnt signaling pathway are essential during embryonic development and promote cell proliferation, differentiation, migration, and growth (Yang 2010 and Le 2014). TGFβ is involved in cell growth and differentiation (Zhao 2014). AhR is a ligand-activated transcription factor that is necessary for xenobiotic metabolism and has been shown to be an upstream activator of murine *Foxq1* and zebrafish *foxq1b* (Planchart and Mattingly 2009). During developmental processes, *FOXQ1* interacts with the Hox gene family, which participates in organogenesis and developmental patterning (Martinez-Ceballos 2005). *FOXQ1* has also been shown to be a downstream target of the retinoic acid pathway. Retinoids are natural analogues of vitamin A, and are necessary for proper embryonic development (Zhuang 2003). The interaction between these pathways and *FOXQ1* contributes to the regulation of gene expression levels necessary for cellular

functions. The following paragraphs summarize what is known about the interactions between FOXQ1 and these pathways and genes.

Hedgehog Signaling: The hedgehog signaling pathway plays an important role in cell growth and maintenance during development and throughout the lifetime of an organism. The transmembrane protein receptor Patched (PTCH1) regulates hedgehog signaling by repressing the G-protein coupled receptor Smoothened (SMO) until the hedgehog protein (Hh) binds to PTCH1, initiating signaling. SMO activation stimulates a downstream signal transduction event that inactivates the intracellular hedgehog pathway regulator SUFU, causing the transcriptional effector GLI to translocate from the cytoplasm to the nucleus where it activates or represses transcription of target genes (Katoh 2008). *In silico* analysis of the rat genome discovered that GLI2 potentially activates many genes in the Fox family, including *Foxq1* (Katoh 2008). However, the significance of this potential interaction remains unknown.

Wnt Signaling: The Wnt signaling pathway is activated throughout embryonic development, but also plays a role in cancer development and progression. The Wnt protein activates signaling by binding to the G-protein coupled receptor Frizzled (Logan and Nusse 2004). The resulting signal transduction cascade stabilizes the effector molecule, β-catenin, and releases it from an intracellular destruction complex. β-catenin then translocates to the nucleus where it binds to the TCF/LEF family of transcription factors and activates transcription of target genes. In the absence of β-catenin, TCF/LEF is bound to the Groucho corepressor and functions instead as a repressor of transcription (Daniels and Weis 2005).

Since both the Wnt signaling pathway and *FOXQ1* are upregulated in colorectal cancer, among others, studies have been performed to determine the cause and effect of this upregulation. It was concluded that *FOXQ1* and Wnt signaling are highly correlated: an increase in Wnt signaling in human colorectal cancer cells leads to an increase in *FOXQ1* mRNA and protein levels, signifying that *FOXQ1* is a downstream target of the Wnt signaling pathway (Christensen 2013), which is supported by the finding that *FOXQ1* contains a TCF-4 binding motif in its promoter region. Chromatin immunoprecipitation (ChIP-seq) experiments, which analyze protein interactions with DNA, found that β-catenin binds to this region of the *FOXQ1* promoter, thus indicating that Wnt signaling directly regulates the expression of *FOXQ1* (Christensen 2013). In Wnt signaling, the protein Groucho mediates transcriptional activity by acting as a corepressor. As discussed below, it appears that FOXQ1 also regulates transcription primarily through repression. Interestingly, FOXQ1 contains two engrailed homology (*eh1*)-like motifs, which are motifs known to mediate interactions with Groucho (Yaklichkin 2007). These results indicate that the Wnt signaling pathway is a direct upstream activator of *FOXQ1* transcription by the binding of β-catenin to *FOXQ1*'s promoter, and that FOXQ1 may interact with the Wnt corepressor Groucho through its *eh1*-like motifs. Further studies would have to be conducted to verify the relationship between FOXQ1 and Groucho.

TGFβ Pathway: TGFβ is involved in bone morphogenesis during development and tissue homeostasis throughout adulthood. TGFβ1 is a type 1 receptor that when activated by the TGFβ ligand, phosphorylates R-Smad proteins, which recruit the intracellular protein

Smad4 and translocate to the nucleus where they regulate transcription of target genes (Zhao 2014). Both TGFβ1 and FOXQ1 have been shown to play a role in epithelial plasticity (that is, the ability of epithelial cells to alter their phenotypic state), and are involved in epithelial-mesenchymal transitions (EMT). During EMT, epithelial cells lose their polarity and become invasive and migratory (Feuerborn 2011 and Zhang 2011). An increase in TGFβ1 signaling in mouse epithelial cells results in an increase in *Foxq1* expression, demonstrating a positive correlation. The transcription factors Zeb1 and Zeb2, which are known targets of the TGFβ1 signaling pathway, enhance EMT during cancer progression (Feuerborn 2011). siRNA knockdown of *Foxq1* expression results in decreased expression of Zeb1 and Zeb2, suggesting *Foxq1* may play a role in TGFβ1 by directly regulating target genes, or by regulating upstream activators or repressors of TGFβ1 targets. Since a decrease in *Foxq1* signaling inhibits TGFβ1-induced EMT in carcinoma, this pathway may be very useful in studying possible cancer therapies (Zhang 2011). These results indicate a clear relationship between TGFβ and *FOXQ1* in both development and carcinogenesis.

Aryl Hydrocarbon Receptor (AhR) Pathway: AhR is a ligand-activated Per-Arnt-Sim (PAS) transcription factor that functions in xenobiotic metabolism, liver development, and hepatocarcinogenesis (Stevens 2009 and Faust 2013). Once a ligand binds, AhR is released from its chaperone complexes in the cytoplasm, where it translocates to the nucleus of the cell. The PAS domain of AhR mediates heterodimerization of AhR to ARNT (aryl hydrocarbon receptor nuclear translocator). This complex binds to specific sequences called dioxin response elements (DREs) in promoter regions, allowing for the transcriptional

activation of genes that are involved in xenobiotic metabolism (Stevens 2009). Potential DREs have been discovered within the promoter region of *FOXQ1* in zebrafish, mice, and humans (Planchart and Mattingly 2010). AhR activity has been shown to increase *foxq1b* expression in zebrafish, the rat hepatoma cell line, H4IIE, and the mouse hepatoma cell line, Hepa-1c1c7, upon exposure to the polycyclic aromatic hydrocarbon 2,3,7,8-tetrachlorodibenzo-*p*-dioxin (TCDD) (Planchart and Mattingly 2010, Dere 2011, Thornley 2011). In 48 hours post fertilization (hpf) TCDD exposed zebrafish, an upregulation of *foxq1b* was localized to the jaw structure known as Meckel's cartilage, which is derived from the first pharyngeal arch (Planchart and Mattingly 2010). In WB-F344 cells, TCDD-activated AhR increases the expression of *Foxq1,* and exposure to the AhR inhibitor CH223191 reduces *Foxq1* mRNA levels (Faust 2013), further demonstrating *Foxq1* is a downstream target of AhR.

Hox Genes: The Hox gene family plays a crucial role in development by regulating processes involving cellular interactions, the cell cycle, and cell death in order to create the structural patterning of the vertebrate body plan (Pearson 2005). Mutations in *Hoxc13*, a member of the Hox gene family, results in mice born with brittle hair that gives way to alopecia (Godwin 1998). An overexpression of *Hoxc13* also causes a delay in hair development and hair loss to occur (Tkatchenko 2001). *Foxq1* is expressed in the hair medulla, the inner most layer of the hair shaft, and if *Foxq1* is mutated, the hair becomes very thin, which is known as the satin hair phenotype (Hong 2001). Transgenic mice overexpressing *Hoxc13* repress transcription of *Foxq1*; however; when *Hoxc13* and *Foxq1*-

luc are co-transfected into NIH3T3 cells or C2C12 myofibroblasts, *Hoxc13* upregulates the expression of *Foxq1* (Potter 2006). Although these results are contradictory, which could be due to cell type or *in vitro* versus *in vivo* studies, luciferase assays indicate that *Hoxc13* binds directly to the *Foxq1* promoter (Potter 2006). Another Hox gene, *Hoxa1*, which is a target of retinoic acid, is an essential gene for correct hindbrain and skull formation. *Foxq1* expression levels increase in an engineered *Hoxa1* double knockout embryonic stem cell line (Martinez-Ceballos 2005), indicating *Hoxa1* is a repressor of *Foxq1* transcription. *FOXQ1* is important for craniofacial development, and its regulation by *HOXA1* could be necessary for proper formation of the craniofacial region.

Retinoic Acid Pathway: Like *Hoxa1*, *Foxq1* has been identified as a downstream target of the retinoic acid (RA) pathway. Retinoic acid binds and activates retinoic acid receptors (RARs α, β, and γ) and retinoid X receptors (RXRs α, β, and γ). The RARs then regulate transcription by binding to retinoic acid response elements (RAREs) in the promoter or enhancer regions of target genes (Zhuang 2003). The RARβ gene contains four isoforms: β_1, β_2, β_3, and β_4, where β_2 is the most abundant and the major RA-inducible isoform. In wildtype F9 teratocarcinoma cells, *Foxq1* mRNA levels increased upon exposure to RA; however, when a homozygous knockout of RARβ_2 was generated in F9 cells, *Foxq1* mRNA levels showed diminished expression (Zhuang 2003). *Foxq1* expression was also low in RARγ homozygous knockout cells (Zhuang 2003), indicating that both retinoic acid receptors mediate the transcriptional activity of *Foxq1*.

FOXQ1 in Development

Embryonic development requires a vast number of genes working together to create every aspect of a properly functioning organism. Early in development, structures called pharyngeal or branchial arches appear in the head region of vertebrate embryos. The arches are populated by migrating neural crest cells that give rise to diverse cell lineages. The evolution of the pharyngeal arches has been highly conserved throughout the development of vertebrate animals. In jawless chordates, such as the lamprey, the pharyngeal skeleton is comprised of cartilage that forms an unjointed branchial basket which supports the gills (Yao 2011). In jawed chordates, such as zebrafish, the first pharyngeal arch forms a jointed jaw (Cerny 2010). The posterior pharyngeal pouches become the thyroid, parathyroid, and thymus, which are structures of great importance to tetrapods (Graham 2005). The conservation of *foxq1* expression in the pharyngeal pouches has been seen throughout evolution.

In situ hybridization using a *foxq1* riboprobe was performed on the jawless chordate model, *Lampetra planeri* (lamprey), for a better understanding of its mRNA localization throughout different stages of development. *Foxq1* mRNA is initially located in the developing pharyngeal pouches, which become openings for the gills (stage 20). By stage 26, it is localized specifically to pouches 1, 5, 6, and 7. Higher resolution studies of embryos at stage 22 demonstrate that *foxq1* expression resides in the pouch endoderm. By stage 29, the lamprey embryo expresses *foxq1* in the posterior ventral region of the gut and in the tail fin area. *In situ* hybridization at stage 30 shows *foxq1* is present in the oral hood, a structure

formed by the continuation of the lips that leads to the mouth, and the branchial basket (Wotton and Shimeld 2011) (for more information on lamprey staging refer to (Piavis 1960)). Other chordates, such as the invertebrates *Amphioxus* and *Ciona*, express *foxq1* in the endostyle, which is a structure that aids in transporting food to the esophagus (Mazet 2005, Ogasawara and Satou 2003).

In the African clawed frog, *Xenopus laevis*, *foxq1* expression appears in the gastrula stage, but is not fully defined until neurulation (Choi 2006) (For more information on *Xenopus* staging, refer to Nieuwkoop and Faber 1994). As *Xenopus* embryos develop, *foxq1* is expressed in the gastrointestinal tract and pharyngeal pouches. *In situ* hybridization of stage 44 *Xenopus* embryos shows *foxq1* is specifically expressed in the tongue, as well as part of the stomach and intestines (Choi 2006). Comparing the role of *foxq1* in the agnatha (jawless) model and the gnathostome (jawed vertebrate) model provides evidence that its restriction to the endoderm and expression in the gastrointestinal system is evolutionarily conserved.

Foxq1 has similar expression profiles in mammalian species as well. *Foxq1* aids in the formation of the canalicular apical membranes within the parietal cells of the stomach. When *Foxq1* expression is deficient, adequate gastric acid secretion is impaired (Goering 2008). The importance of *Foxq1* expression in stomach function has been shown in knockout experiments in mice. Foveolar cells line the stomach and protect it from corrosive gastric acid damage by secreting mucins. Loss of *Foxq1* expression alters foveolar cell function resulting in decreased expression of the stomach mucin gene, *Muc5ac*, and loss of stomach

mucin (Verzi 2008). These results show that *Foxq1* plays an important role in gastric function through the regulation of acid and mucin secretion.

Craniofacial development is also regulated by *Foxq1*, as seen in the *Foxq1* mouse knockout. The *Foxq1* deficient mutant mouse embryos displayed head abnormalities due to a smaller brain vesicle, which could have been the result of decreased cerebrospinal fluid volume. Transverse sections of the forebrain that were stained with hematoxylin-eosin revealed shrinkage of the third and lateral ventricles (Goering 2008). *Foxq1* deficient mice also have a greater chance of mortality; however, upon examining the deceased embryos, the liver, heart, and placenta were all normal compared to wild-type and *Foxq1* hemizygotes. The cause of lethality is unknown but restricted to *Foxq1* deficient offspring from crosses between C57BL/6J X 129/Sv (Goering 2008). Preliminary data in our lab has shown that *foxq1b* knockdown in zebrafish also causes craniofacial abnormalities, specifically in the developing jaw.

Foxq1 plays a role in hair follicle development, as described previously. A deletion in the *Foxq1* gene results in the satin hair mutation (Hong 2001). Satin hair is shinier and thinner than that of wild type mice, and its appearance is due to increased fibrous material and the inability to keratinize correctly. Since *Foxq1* acts directly on the matrix cells, which differentiate into the outgrowing hair shaft and inner root sheath (Driskell 2011), its abnormal expression is responsible for altering normal hair follicle development (Hong 2001).

Foxq1 is involved in smooth muscle development by repressing the transcription of smooth muscle-specific telokin, smooth muscle α, and smooth muscle myosin by directly binding to the forkhead consensus sites located on their promoters (Hoggatt 2000). Since *Foxq1* expression is mostly found in epithelial cells, it was suggested that its role is to negatively regulate the transcription of smooth muscle genes in cell types other than smooth muscle, thereby restricting their expression to smooth muscle cells (Hoggatt 2000). *FOXQ1*'s involvement in gastric acid secretion, hair follicle formation, craniofacial patterning, and smooth muscle regulation indicates its vital role in various aspects of development.

FOXQ1 **induces Epithelial-Mesenchymal Transition (EMT)**

Epithelial cells form a protective barrier against bacteria, prevent substances from leaving their internal environment, and regulate absorption and secretion of fluids in the gut (McConnell 2005). Their properties include, cell adhesion, polarity, and stationary properties, all of which are lacking in mesenchymal cells. Mesenchymal cells, on the other hand, are important during embryogenesis and during the wound healing process due to their ability to migrate; however, the process of epithelial-mesenchymal transition (EMT), where epithelial cells lose their cell adhesion and develop the migratory properties of mesenchymal cells, can result in a stem cell-like form that acquires invasive and mobile abilities leading to tumor formation and cancer development (Li 2015). Recent studies suggest that *FOXQ1* has the capability to influence EMT (Feuerborn 2011) and therefore, *FOXQ1* may contribute to growth and metastasis of malignant tumors.

E-cadherin is an adherens junction protein that is an important component of the epithelium because of its involvement with cell adhesion and maintenance of epithelial cell polarity (Gumbiner 1996). β-catenin and γ-catenin are proteins that also play roles in cell adhesion. Epithelial cells that downregulate E-cadherin, β-catenin, and γ-catenin exhibit a fibroblast-like phenotype characterized by detachment and dispersion from the basement membrane (Zhang 2011 and Qiao 2011). Fibronectin, Vimentin, and N-cadherin, on the other hand, are known markers of mesenchymal cells. When ectopic *FOXQ1* expression is induced in the human mammary cell line, HMLE, the cells appear spindle-like compared to control cells, and E-cadherin, β-catenin, and γ-catenin are downregulated, whereas Fibronectin, Vimentin, and N-cadherin are upregulated, signaling the beginning of EMT. However, when *FOXQ1* is overexpressed in the MDCK cell line, E-cadherin expression decreases but no other epithelial or mesenchymal markers are affected (Zhang 2011). The varying epithelial and mesenchymal cell marker expression seen in the HMLE and the MDCK cells could be due to different cell properties. However, these results indicate *FOXQ1* is important for regulating genes associated with EMT, specifically genes associated with cell adhesion. A decrease in *FOXQ1* expression leads to an increase in cell size, as well as an increase in E-cadherin and β-catenin, and a decrease in Vimentin, similar to what is observed during mesenchymal-epithelial transition (MET), where migratory mesenchymal cells transition to a stationary, epithelial-like state (Feuerborn 2011 and Zhang 2011). Downregulation of *FOXQ1* in MDA-MB-231 cells also converts the mesenchymal spindle-like cell structure to an epithelial-like state, and cell adhesion is restored (Qiao 2011). From

the standpoint of cancer therapy, pharmacologic inhibition of *FOXQ1* could be used as a strategy in the fight against cancer.

Several transcription factors such as Snail1, Snail2, Twist1, E47, Zeb1, and Zeb2 are overexpressed in carcinomas and induce EMT by inhibiting E-cadherin expression (Zhu 2013). These transcription factors bind to the E-box region of the E-cadherin promoter, downregulating its transcription and promoting EMT (Zhu 2013). Since *FOXQ1* overexpression also decreases the expression of E-cadherin, a study was performed to determine if *FOXQ1* and E-cadherin directly interact. Using ChIP-seq, FOXQ1 was found to bind the E-box region of the E-cadherin promoter (Zhang 2011). These results imply that *FOXQ1* overexpression activates EMT in a similar manner as the EMT transcription factors by directly repressing E-cadherin transcription.

The EMT transcription factors, Twist1 and Zeb2, have been identified as downstream targets of *FOXQ1*. Three potential binding sites for FOXQ1 have been discovered in the Twist1 promoter, and two in the Zeb2 promoter through *in silico* analysis (Meng 2014). Although FOXQ1 promotes EMT by acting as a repressor of E-cadherin, it also may promote EMT by acting as an activator of Twist1 and Zeb2 (Abba 2013 and Xia 2014).

Platelet-derived growth factor receptors PDGFRα and β are tyrosine kinase receptors involved in cell proliferation, differentiation, and growth, as well as the development of cancer by contributing to TGFβ-induced EMT maintenance (Jechlinger 2006). FOXQ1, Twist1, and Zeb2 all have the capability to regulate PDGFRα and β, indicating that FOXQ1 acts directly or indirectly (through Twist1 and Zeb2) on PDGFRα and β activation. When

either PDGFRα or β is silenced in HMLE/FOXQ1 cells (where *FOXQ1* is overexpressed), there is a decrease in *FOXQ1*-induced cell migration and invasion in a Transwell migration assay; however, EMT is not reversed (Meng 2014). This indicates that PDGFRα and β may play a role in the maintenance of EMT, but other genes are involved in the activation of EMT.

When epithelial cells transition to a mesenchymal phenotype, they acquire stem cell traits that allow them to develop invasive and migratory properties. In carcinomas, metastasis occurs when tumor cells from one organ attack a distant organ in the body, which is the most common cause of death by carcinomas (Zhang 2011 and Qiao 2011). Depleting *FOXQ1* in a human mammary metastatic cell line increases the apoptotic response to 5-FU, paclitaxel, and CPT chemotherapy agents (Qiao 2011). *FOXQ1*'s effect on chemoresistance was studied in the human mammary epithelial cell line HMLE/FOXQ1, in which *FOXQ1* is ectopically overexpressed. When treated with two chemotherapy agents, doxorubicin and paclitaxel, cells aberrantly expressing *FOXQ1* exhibit significantly greater survival than cells in which PDGFRα or β was knockdown leading to a decrease in *FOXQ1*-promoted oncogenesis (Meng 2014). *FOXQ1* overexpression also inhibits benzyl isothiocyanate (BITC), which is a naturally occurring product found in cruciferous vegetables that has been shown to reduce mammary cancer in mice, and pancreatic atypical hyperplasia and adenocarcinoma in hamsters (Warin 2009 and Kuroiwa 2006). In breast cancer cells, BITC has been shown to inhibit TGFβ1-induced EMT (Sehrawat 2011). BITC decreases the aggressiveness of carcinoma by increasing the expression of E-cadherin. It also suppresses the mesenchymal

marker Vimentin and the E-cadherin repressors Slug and Snail. BITC increases cell adhesion in breast cancer cells compared to control cells. However, the overexpression of *FOXQ1* makes it more difficult for BITC to increase E-cadherin protein levels or suppress Vimentin (Sehrawat 2013). These results further demonstrate the impact *FOXQ1* has on the resistance against chemotherapies. Therefore, repressing expression of *FOXQ1* could be beneficial in these treatments by increasing cancer cell apoptosis, and reverting mesenchymal cells back to an epithelial-like state in order to regain cell adhesion and epithelial cell properties.

Other Roles of *FOXQ1* in Carcinoma

According to the American Cancer Society, there were approximately 1.7 million new cancer cases that led to almost 600,000 deaths in the United States in 2014 (Siegel 2014). *FOXQ1* expression is necessary for proper embryonic development, but research has shown that its aberrant expression in adulthood plays a role in cancer formation and progression, as described in the preceding section.

Overexpression of *FOXQ1* is present in colorectal cancer, breast cancer, pancreatic cancer, and many others. *FOXQ1* has been shown to play a role in the cell cycle, which can influence cell proliferation (Gao 2012). It can also affect caspase activity, leading to a decrease in apoptosis (Kaneda 2010). A few microRNAs have been shown to be downregulated by *FOXQ1* overexpression (Peng 2014). MicroRNAs (miRNAs) are small non-coding RNAs that regulate protein production by down-regulating gene expression through mRNA degradation or translational termination. *FOXQ1*'s involvement in the cell

cycle, interaction with the immune system, regulation of miRNAs, and relationship with other cellular factors may contribute to the formation, growth, and metastasis of cancer.

The *in vitro* overexpression of *FOXQ1* increases migration and invasion of bladder cancer, breast cancer, lung cancer, and colorectal cancer (Zhu 2013, Zhang 2011, Feng 2014, and Abba 2013). In colorectal cancer, *FOXQ1* upregulation caused an increase in VEGFA, WNT3A, RSPO2, and BCL11A genes, which are all known to play a role in tumor growth (Kaneda 2010). RSPO2 has also been shown to be an upstream activator of Wnt signaling and play a role in craniofacial patterning (Jin 2011), further signifying a relationship with *FOXQ1*. Although overexpression leads to angiogenic and anti-apoptotic properties in colorectal cancer, *FOXQ1* does not affect tumor stage, grade, localization or metastatic status of this particular cancer (Kaneda 2010, Christensen 2013). Interestingly, overexpression of *FOXQ1* in colorectal cancer was not associated with EMT (Christensen 2013). In glioblastoma, *FOXQ1* represses neurexin (NRXN3), which is important for cell adhesion and recognition. The repression of NRXN3 caused an increase in proliferation and migration of tumors called gliomas in the central nervous system (Sun 2013). *FOXQ1* is also upregulated in nasopharyngeal cancer, and its expression was lowest in clinical stage I and tumor stage T1, but increased in clinical stage II-IV and T2-T4 (clinical stage indicates degree or spread of cancer and tumor stage (T) indicates size and growth of tumor) (Peng 2014). This indicates that *FOXQ1* may play a role in the severity of nasopharyngeal cancer and tumor size, but further studies would have to be conducted to know for certain. *FOXQ1* has also been shown to be upregulated in metastatic hepatocellular carcinoma (HCC) when compared

to non-metastatic HCC (Xia 2014*). FOXQ1* has the highest expression in gastric, colorectal, and lung cancer, and its overexpression has been shown to influence aggressive cell properties in a variety of cancer types (Kaneda 2010).

The cell cycle, which consists of a series of events that lead to cell replication and division, is maintained by checkpoints, called G1 and G2, which halt the cell cycle if any DNA damage is detected. *FOXQ1* is important for cell proliferation by assisting in the G1-phase of the cell cycle (Gao 2012). When *FOXQ1* is repressed, cells are more likely to remain in the G0 and G1 phases, and fewer cells are seen transitioning to S-phase, G2, and Mitosis (Feuerborn 2011). Cyclin-dependent kinases CDK4 and CDK6 are required for movement of cells from G1 to S-phase. When *FOXQ1* is repressed in mammary gland cells, the protein levels of CDK4 and CDK6 decrease (Feuerborn 2011), and cyclin-dependent kinase inhibitors $p27^{Kip1}$ and $p21^{Cip1}$ increase, consistent with the hypothesis that *FOXQ1* may be involved in cell cycle regulation (Gao 2012). Contradictory results were seen in a colorectal cell line, where p21 is upregulated when *FOXQ1* is overexpressed, which could be due to different cell types, cancer types, or mechanisms (Kaneda 2010). The p21 promoter contains a FOXQ1 binding site, where binding of FOXQ1 activates p21 transcription (Kaneda 2010). The increase of p21 by FOXQ1 in colorectal cancer results in resistance to the induction of apoptosis by DNA damage, but does not appear to contribute to FOXQ1-mediated tumor growth (Kaneda 2010). Further research should be performed to determine whether *FOXQ1* acts as a repressor or an activator of p21, or if these regulation differences are cancer specific.

Numerous caspases are activated in cells undergoing apoptosis (Chen and Wang 2002). Caspase activity was measured in ovarian carcinoma SKOV3 cells in order to study *FOXQ1*'s role in apoptosis. The activity of caspase 3 and 7 increases 48 hours after *FOXQ1* expression is knocked down indicating *FOXQ1* may have anti-apoptotic functions (Gao 2012). Similar results are seen in colorectal cells, where the overexpression of *FOXQ1* leads to a decrease in caspase 3 expression (Kaneda 2010). Ectopic *FOXQ1* expression also diminished polyADP ribose polymerase (PARP), which detects single stranded DNA breaks, as well as signals for repair (Qiao 2011), both of which may contribute to the anti-apoptotic characteristics of *FOXQ1*. These results indicate that decreasing *FOXQ1* expression might be useful at increasing apoptosis driven by chemotherapy drugs.

FOXQ1 can contribute to cancer through its interactions with components of the immune system. Tumor-associated macrophages (TAMs) are derived from circulating monocyte precursors when chemoattractants from tumor and stromal cells are secreted (Xia 2014). TAMs secrete the proinflammatory chondroitin sulfate proteoglycan, VersicanV1, which stimulates macrophages to produce tumor necrosis factor-α (TNF-α); TNF-α is known to induce metastasis in hepatocellular carcinoma (HCC) (Xia 2014). When VersicanV1 is upregulated in HCC, migration and invasion are increased. Overexpression of *FOXQ1* upregulates VersicanV1 expression through direct binding of *FOXQ1* to the *VCAN* promoter, which has been shown to increase macrophage infiltration and metastasis (Xia 2014). This indicates that *FOXQ1*'s role in the immune system could be a major contributor to cancer progression.

When miRNAs are aberrantly expressed, they can either play a role in tumor suppression or tumor progression. Several miRNAs have been found to regulate *FOXQ1*. For example, direct regulation of *FOXQ1* mRNA by miR-124 resulting in reduced FOXQ1 expression levels was observed in nasopharyngeal carcinoma (NPC), which decreased migration and invasion of NPC cells (Peng 2014). A similar study was conducted on the relationship between miRNA-422a and *FOXQ1* in HCC, where miR-422a overexpression was shown to diminish *FOXQ1* expression. On the other hand, *FOXQ1* overexpression decreased miR-422a levels via a negative feedback loop. ChIP-PCR showed no interaction between FOXQ1 and the promoter region of miR-422a, indicating that this effect is indirect (Zhang 2015). These results demonstrate that miR-124, miR-422a, and potentially other miRNAs, are tumor-suppressors and their activation could be useful targets in chemotherapy by downregulating genes, like *FOXQ1,* that are overexpressed in cancer.

Conclusion

Forkhead box genes are important for cell function and survival. The transcription factor *FOXQ1* is the downstream target of many signaling pathways that regulate its expression throughout development and carcinogenesis. *FOXQ1* is involved in several aspects of development including craniofacial, gastrointestinal, and hair follicle structure. Its role in the activation of EMT, disruption of the cell cycle, and resistance to apoptosis leads to the formation and progression of carcinoma. Although *FOXQ1* is not the only misregulated gene in disease progression, knowledge of its properties and function will be useful for treatment and prevention methods.

Table 1: Forkhead Box (Fox) Gene Subfamily Members. Each subfamily symbol, approved name, synonyms, human chromosome location, and protein size are listed. If a subfamily member contains more than one isoform it is also listed along with its protein size. This collection was compiled using the National Center for Biotechnology Information website.

Approved Symbol	Approved Name	Synonyms	Human Chromosome Location	Number of Amino Acids
FOXA1	forkhead box A1	HNF3A, TCF3A	14q21.1	472
FOXA2 isoform 1	forkhead box A2	HNF3B, TCF3B	20p11	463
FOXA2 isoform 2				457
FOXA3	forkhead box A3	HNF3G, FKHH3, TCF3G	19q13.32	350
FOXB1	forkhead box B1	HFKH-5, FKH5	15q22.2	325
FOXB2	forkhead box B2	bA159H20.4	9q21.2	432
FOXC1	forkhead box C1	ARA, IGDA, IHG1, FKHL7, IRID1, RIEG3, FREAC3, FREAC-3	6p25	553
FOXC2	forkhead box C2	FKHL14, MFH-1, MFH1, LD	16q24.1	501
FOXD1	forkhead box D1	FKHL8, FREAC4, FREAC-4	5q13.2	465
FOXD2	forkhead box D2	FKHL17, FREAC9, FREAC-9	1p34-p32	495
FOXD3	forkhead box D3	Genesis, HFH2, AIS1, VAMAS2	1p31.3	478
FOXD4	forkhead box D4	FKHL9, FREAC5, FREAC-5, FOXD4A	9p24.3	439
FOXD5	forkhead box D5	FOXD4L1, bA395L14.1	2q13	408
FOXD6	forkhead box D6	FOXD4L3	9q21.11	417
FOXE1	forkhead box E1	FKHL15, TITF2, FOXE2, TTF2, TTF-2, HFKH4, HFKL5	9q22	373
FOXE3	forkhead box E3	FKHL12, FREAC8	1p32	319
FOXF1	forkhead box F1	FKHL5, FREAC1, ACDMPV	16q24	379
FOXF2	forkhead box F2	FKHL6, FREAC2, FREAC-2	6p25.3	444
FOXG1	forkhead box G1	BF1, BF2, QIN, FKH2, HBF2, HFK1, HFK2, HFK3, KHL2, FHKL3, FKHL2, FKHL3, FKHL4, HBF-1, HBF-2, HBF-3, FOXG1A, FOXG1B, FOXG1C, HBF-G2	14q13	489
FOXH1	forkhead box H1	FAST1, FAST-1	8q24.3	365
FOXI1 isoform a	forkhead box I1	HFH3, FKH10, HFH-3, FKHL10, FREAC6, FREAC-6	5q34	378
FOXI1 isoform b				283
FOXI2	forkhead box I2	FLJ46831	10q26.2	318
FOXJ1	forkhead box J1	FKHL13, HFH-4, HFH4	17q25.1	421
FOXJ2	forkhead box J2	FHX	12p13.31	562
FOXJ3 isoform 1	forkhead box J3	KIAA1041	1p34.2	622
FOXJ3 isoform 2				588
FOXK1	forkhead box K1	FOXK1L	7p22.1	733
FOXK2	forkhead box K2	ILF, ILF1, ILF-1	17q25	660
FOXL1	forkhead box L1	FKHL11, FREAC7, FKH6	16q24	345
FOXL2	forkhead box L2	BPES, BPES1, PFRK, POF3, PINTO	3q23	376
FOXM1 isoform 1	forkhead box M1	MPP2, TGT3, HFH11, HNF-3, INS-1, MPP-2, PIG29, FKHL16, FOXM1B, HFH-11, TRIDENT, MPHOSPH2	12p13	801
FOXM1 isoform 2				763
FOXM1 isoform 3				748
FOXM1 isoform 4				748
FOXM1 isoform 5				747

Table 1 Continued

FOXN1	forkhead box N1	WHN, RONU, FKHL20	17q11-q12	648
FOXN2	forkhead box N2	HTLF	2p22-p16	431
FOXN3 isoform 1	forkhead box N3	C14orf116, CHES1, PRO1635	14q31.3	490
FOXN3 isoform 2				468
FOXN4	forkhead box N4		12q24.11	517
FOXN5	forkhead box N5	FOXR1, DLNB13	11q23.3	292
FOXN6	forkhead box N6	FOXR2	Xp11.21	311
FOXO1	forkhead box O1	FKHR, FOXO1A, FKH1	13q14.11	655
FOXO3	forkhead box O3	FOXO3A, AF6q21, FKHRL1, FKHRL1P2, FOXO2	6p21	673
FOXO4 isoform 1	forkhead box O4	MLLT7, AFX, AFX1	Xq13.1	505
FOXO4 isoform 2				450
FOXO6	forkhead box O6		1p34.2	492
FOXP1 isoform 1	forkhead box P1	MFH, QRF1, 12CC4, hFKH1B, HSPC215	3p14.1	677
FOXP1 isoform 2				114
FOXP1 isoform 3				676
FOXP1 isoform 4				693
FOXP1 isoform 5				601
FOXP1 isoform 6				577
FOXP1 isoform 8				679
FOXP2 isoform 1	forkhead box P2	TNRC10, SPCH1, CAGH44	7q31	715
FOXP2 isoform 2				740
FOXP2 isoform 3				432
FOXP2 isoform 4				732
FOXP2 isoform 5				714
FOXP2 isoform 6				457
FOXP3 isoform a	forkhead box P3	IPEX, JM2, XPID, AIID, PIDX, DIETER	Xp11.23	431
FOXP3 isoform b				396
FOXP4 isoform 1	forkhead box P4	hFKHLA	6p21.1	680
FOXP4 isoform 2				667
FOXP4 isoform 3				678
FOXQ1	forkhead box Q1	HFH1	6p25	403
FOXR1	forkhead box R1	DLNB13, FOXN5	11q23.3	292
FOXR2	forkhead box R2	MGC21658, FOXN6	Xp11	311
FOXS1	forkhead box S1	FKHL18, FREAC10	20q11.21	330

II. DESIGN, CONSTRUCTION AND PRELIMINARY CHARACTERIZATION OF A MYC-TAGGED ALLELE OF THE ZEBRAFISH FORKHEAD BOX GENE, *foxq1b*

Abstract

Colorectal, pancreatic, and breast cancer are among the top five most deadly cancers. The transcription factor *FOXQ1* is significantly upregulated in these cancers, yet many of the genes directly regulated by FOXQ1 are still unknown. Through preliminary research, our lab uncovered several genes upregulated in a *foxq1b* morphant, in which *foxq1b* was knocked down using a gene-specific morpholino. Since there are discrepancies with data generated through the use of morpholinos, a myc-tag sequence was engineered onto the C-terminus of the zebrafish *foxq1b* open reading frame in order to evaluate the previously acquired data utilizing chromatin immunoprecipitation by way of an anti-myc antibody. A transgenic fish, Tg(*foxq1b*:foxq1b-myc), was created that successfully transmitted the myc-tagged *foxq1b* allele, under the control of the endogenous *foxq1b* promoter, to its offspring. We confirmed that the transgenic DNA was transcribed successfully and that the resulting mRNA was translated into protein. This transgenic zebrafish line will be useful for characterizing genes directly regulated by foxq1b and assist in the analysis of other datasets, including those generated from morpholino knockdown of *foxq1b*. Tg(*foxq1b*:foxq1b-myc) will also be useful in characterizing AhR binding sites within the *foxq1b* promoter. AhR directly upregulates *foxq1b*, potentially by binding to regions within the promoter. Although potential binding sites have been speculated, the exact location is still unknown. This knowledge will

benefit the scientific community by providing greater insight into the interactions of genes associated with known developmental pathways and cancer.

Introduction

One in four deaths in the United States is due to cancer, making cancer an enormous public health concern (Siegel 2014). Cancer was the leading cause of death for both men and women ages 40 and above in 2010, and it is estimated that there are over 4,500 new cancer diagnoses every day (Siegel 2014). Colorectal, pancreatic, and breast cancer are among the top five cancers that led to death in 2010. Although cancer death rates have continued to decline over the past 20 years (Siegel 2014), much is still unknown about the molecular and cellular mechanisms involved in cancer development and progression. Learning more about these mechanisms could aid in the discovery of new treatments and improved therapies for this disease.

Human forkhead box Q1 (FOXQ1) is a 403 amino acid transcription factor that contains a winged helix DNA binding domain, similar to other Fox gene family members (Carlsson and Mahlapuu 2002, Bieller 2001 and Hong 2001). FOXQ1 plays an important role in embryonic developmental processes including craniofacial development (Goering 2008), hair follicle formation (Driskell 2011), and gastrointestinal development (Verzi 2008). Overexpression of FOXQ1 has been found in many cancer types, including colorectal (Christensen 2013), pancreatic (Bao 2014), and breast cancer (Zhang 2011). Its involvement in cancer may be attributed to its ability to transcriptionally regulate genes involved in apoptosis (Kaneda 2010), EMT (epithelial-mesenchymal transition) (Feuerborn 2011), and

the cell cycle (Kaneda 2010 and Feuerborn 2011). However, the genes directly regulated by FOXQ1 are still largely unknown.

Zebrafish have become a useful model organism for studying human development and disease. During its evolutionary history, zebrafish underwent a genome duplication resulting in two paralogs, called *foxq1a* and *foxq1b*, orthologous to mammalian *FOXQ1*. In zebrafish, *foxq1b* is upregulated through the AhR pathway when exposed to 2,3,7,8-tetrachlorodibenzo-*p*-dioxin (TCDD). However, no significant changes in *foxq1a* expression were observed upon TCDD exposure (Planchart and Mattingly 2010). In the mouse derived cell line, Hepa-1C1C7, *foxq1* mRNA expression also significantly increased when exposed to TCDD (Thornley 2011). These results appear to suggest that zebrafish *foxq1b* more closely resembles the ancestral form of *Foxq1*, while *foxq1a* may have undergone neofunctionalization. The foxq1b protein is 312 amino acids in size, and its protein sequence is similar to human FOXQ1.

Preliminary research using *foxq1b* morphant zebrafish, in which *foxq1b* was knocked down using antisense morpholinos, indicates that downregulating *foxq1b* results in upregulation of several genes involved in apoptosis and the cell cycle (Table 2). A few of the genes upregulated by knock down of *foxq1b* are *Rbl2*, *Tp53*, *Eda2r*, and *Mdm2*. *Rbl2*, also known as *p130*, is a gene associated with the regulation of the G_0 to G_1 transition of the cell cycle (Jackson 2005). *Rbl2* is also important for the transcriptional regulation of genes involved in the G_2 phase of the cell cycle (Jackson 2005). Another gene upregulated in the *foxq1b* morphant was *Tp53*. *Tp53*, like *Rbl2*, aids in cell cycle arrest at the G_1 or G_2 phase, as

well as apoptosis in response to DNA damage (Agarwal 1995). *Tp53* acquires a spectrum of mutations in the presence of cancer, which interfere with its regulatory mechanisms (Bennett 1999). *Tp53* contains numerous isoforms, one of which is *Δ133p53*, found in humans and zebrafish. The full-length *tp53* has been shown to transactivate the *Δ113p53* isoform, which then antagonizes tp53-induced apoptosis creating a negative feedback loop (Chen 2009). Interestingly, in the *foxq1b* morphant data the *Δ113p53* isoform is most significantly upregulated (44 fold) when *foxq1b* is knockdown, while the full-length *tp53* is not strongly affected (2.3-fold upregulation). *Eda2r*, a gene significantly upregulated in the *foxq1b* morphant, is important during hair and sweat gland development in mammals (Kere 1996), regulation of ectodermal function, and induction of cell death (Brosh 2010). *Eda2r* is a known downstream target of *p53*, and is activated by *p53* in cancer cells where it induces anoikis (Brosh 2010). Anoikis is a type of apoptosis in epithelial cells in response to detachment from the surrounding matrix (Wazir 2015), which occurs during EMT. The oncogene *Mdm2*, which is upregulated by the knockdown of *foxq1b*, is known for its anti-apoptotic effect through negative regulation of *p53* (Momand 1992). The morphant data reveal that *foxq1b* is a negative regulator of the transcription of these genes, which correlates with the hypothesis that *foxq1b* is primarily a repressor of transcription.

Although the preliminary data gathered through the use of *foxq1b* morpholinos is beneficial, there have been many inconsistencies with data collection using this method due to the possibility of off-target effects. The generation of a *foxq1b-myc* construct will assist in

further analysis of data derived from the *foxq1b* morphant, as well as characterize genes that are regulated directly by *foxq1b*.

The *foxq1b-myc* construct can also be useful in characterizing AhR binding site location on the *foxq1b* promoter. 2,3,7,8-tetrachlorodibenzo-*p*-dioxin (TCDD), also known as dioxin, is a polychlorinated compound that has been shown to activate the aryl hydrocarbon receptor (AhR). Zebrafish exposed to TCDD causes upregulation of *foxq1b* mRNA. A program called MatInspector (Genomatrix) was used to analyze 7 kilobases (kb) upstream from the zebrafish *foxq1b* transcription start site (TSS), and found seven potential AhR binding sites, called dioxin response elements (DRE) (Planchart and Mattingly 2010), which are located at -371, -1330, -1349, -4627, -5637, -7,060, and -7,425. DREs contain a core binding site consisting of the sequence: 5'-CGTG-3' (Lusska 1993). Since the Tg(*foxq1b*:foxq1b-myc) zebrafish only contain the 5kb *foxq1b* promoter region, the *foxq1b-myc* expression level upon exposure to TCDD will further characterize the location of AhR binding to the *foxq1b* promoter.

In this chapter, the design and construction of a vector carrying a myc-tagged allele of *foxq1b* under the control of a 5 kb fragment of the *foxq1b* promoter, as well as the generation and characterization of the transgenic founder carrying this novel allele are described. The use and importance of the construct will also be discussed.

Table 2: Knockdown of foxq1b increases expression of genes involved in the apoptotic pathway. Next generation sequencing (NGS) and RT-qPCR were used to generate a list of genes that increased expression in *foxq1b* morphants compared to wild-type zebrafish. The majority of the genes are proapoptotic. *tp53**: The induction of full length *tp53* and its isoform *Δ113p53* from qPCR analysis is shown. The induction of both the full length and isoform combined from NGS analysis is shown. *mdm2* (in red): only anti-apoptotic gene generated by NGS. (Preliminary research conducted by the Planchart Lab).

Gene Symbol	Gene Name		Foxq1b Morphant v. WT
			NGS
eda2r	ectodysplasin A2 receptor (Xedar)		31
fos	FBJ osteosarcoma oncogene		21
bbc3	BCL2 binding component 3 (PUMA)		19.2
rbl2	retinoblastoma-like 2 (p130)		17.1
casp8	caspase 8		18.4
phlda3	pleckstrin homology-like domain, family A, member 3		17.7
ccng1	cyclin G1		7.4
*tp53**	transformation related protein 53	*Combined (NGS)*	11.2
		Full-length (qPCR)	2.3
		Δ113p53 (qPCR)	44
cdkn1a	cyclin-dependent kinase inhibitor 1A (p21)		10.6
mdm2	transformed mouse 3T3 cell double minute 2		11.3

Materials and Methods

DNA preparation from Glycerol Stock

A fosmid (CH1073-460D17) was propagated in *E. coli* from a glycerol stock by streaking it on an agar plate supplemented with chloramphenicol (SIGMA C-0857) (12.5µg/ml) and incubating it for 20 hours at 37° C. CH1073-460D17 harbors an approximately 6 kb fragment containing the promoter region (~5 kb) and open reading frame of zebrafish *foxq1b*. A single colony was cultured in a 15ml culture tube containing 2ml Lysogeny Broth (LB; 10g NaCl, 10g Tryptone, and 5g yeast extract in 1L of water adjusted to pH 7.5 and autoclaved) supplemented with 12.5µg/ml chloramphenicol for 20 hours at 37º C and 250 rpm. A mini-prep of the culture was performed using the QIAGEN Plasmid Mini kit (Cat. 12123). A restriction digest using *Hind*III (NEB Cat. R0104S) was performed in order to confirm that the fosmid carried the desired insert. Briefly, 3µl 10X buffer, 21µl water, 5µl mini-prep DNA (776ng/µl) and 1µl of enzyme were gently mixed by pipetting and incubated in a 37º C water bath for 4 hours. The digest was analyzed on a 0.8% agarose gel.

Engineering and cloning of foxq1b promoter sequence

All primers were purchased from Integrated DNA Technologies (IDT) and sequences are shown in Table 3. Forward (zf_*foxq1b_Kpn*I_Prom_L) and reverse (zf_*foxq1b_Not*I_3UTR_R) primers were designed to flank the 5.2kb *foxq1b* promoter region with *Kpn*I and *Not*I restriction enzyme sites on the 5' and 3' ends, respectively. PCR amplification of the *foxq1b* promoter was as follows: 19µl water, 6µl 5X Phusion HF Buffer, 1.5µl forward primer (10µM stock), 1.5µl reverse primer (10µM stock), 1µl of a 1:10 dilution

of mini-prep DNA (77.6ng/µl), 0.3µl Phusion DNA Polymerase (NEB Cat. M0530S), and 0.6µl dNTPs (10mM stock) were assembled in PCR reaction tubes. The thermal cycling conditions used were: 93° C x 2 minutes; 30 cycles at 93° C x 30 seconds, 55° C x 30 seconds, 72° C x 5 minutes; 72° C x 10 minutes. Amplification products were visualized on a 0.8% agarose gel and the correct amplicon was gel-extracted using a QIAGEN QIAquick Gel Extraction kit (Cat. 28704).

The extracted amplicon and pBluescriptII/SK+ vector (modified to contain I-*Sce*I sites flanking the multiple cloning site) were digested with *Kpn*I HF (NEB Cat. B7204) and *Not*I HF (NEB Cat. R3142L) as described previously, and linearization of the vector was confirmed on a 0.8% agarose gel. Digests were phenol-chloroform extracted by adding 1X TE Buffer to bring the digests to 100µl, followed by 100µl of buffer-saturated phenol-chloroform (SIGMA Cat. P3803). The tubes were vortexed for 30 seconds followed by centrifugation for 5 minutes at 14K rpm. The aqueous phase was transferred to a new tube and 10µl (1/10th of volume) of 3M Sodium Acetate (pH 5.0) (Fisher Scientific Cat. 127-09-3) was added to each tube and vortexed. Afterwards, 300µl (3 volumes) of 100% Ethanol was added to each tube, mixed and chilled on ice for 15 minutes. The tubes were centrifuged at maximum speed (14.8K rpm) for 8 minutes and the supernatant was discarded. The pellets were briefly washed with 500µl 70% Ethanol and centrifuged for 5 minutes, after which the supernatant was discarded. The pellets were dried, and resuspended in 10µl water. A ligation reaction containing the digested *foxq1b* promoter and linearized pBluescriptII/SK+ vector was performed by adding 1µl of the vector (9ng/µl), 6µl of digested *foxq1b* promoter

(2.1ng/µl), 1µl T4 Ligase (NEB Cat M0202S), 1.5µl 10X T4 Buffer, and 5.5µl water. The ligation reactions were incubated in the thermal cycler at 15° C for 16 hours. A transformation was carried out by thawing 50µl of C2925 cells (NEB Cat C2925I) on ice for 10 minutes, then adding 1µl of the ligation reaction to the cell tube and flicking gently to mix. The tubes were placed on ice for 30 minutes, heat shocked for 45 seconds in a 42° C water bath and immediately placed back on ice for 5 minutes. 200µl of room temperature S.O.C. Outgrowth Medium (NEB Cat. B9020S) was added to each tube, and the tubes were incubated for 1 hour at 37° C and 250 rpm. 200µl of each tube were spread on pre-warmed agar plates supplemented with 100µg/ml Ampicillin (SIGMA Cat. A5354), and incubated at 37° C for 16 hours. Single colonies were placed in culture tubes containing 2ml LB supplemented with 100µg/ml Ampicillin, and incubated for 20 hours at 37° C and 250 rpm. Mini preps were performed to isolate the plasmid DNA following the QIAGEN mini kit protocol, and digested with *Kpn*I HF and *Not*I HF, as previously described. One clone with the correct insert was selected and production was scaled up by inoculating 500mL of LB supplemented with ampicillin and culturing as described. A glycerol stock was made containing 700µl of the bacterial culture, 150µl LB, and 150µl glycerol (Fisher Scientific Cat. 56-81-5), and stored at -80° C. Plasmid was purified from the remaining culture using the QIAGEN maxi kit (QIAGEN Cat. 12163) as described by manufacturer. We confirmed the sequence of the *foxq1b* promoter inserted into pBluescriptII/SK+ (referred to as pBS_*foxq1b*P) by Sanger sequencing at the Genomic Services Lab (GSL; NC State) per their protocol.

Engineering and cloning of foxq1b open reading frame and myc-tag sequence

Forward (zf_foxq1b_*Not*I_m-2ORF_L) and reverse (zf_foxq1b_*Sac*I_m-2ORFmyc_R) primers were designed to flank the 864bp *foxq1b* open reading frame, with *Not*I and *Sac*I restriction sites, respectively. The reverse primer contained a myc-tag sequence upstream of the *Sac*I site. A PCR was performed as described above using 390ng of fosmid DNA and the following thermal cycling conditions: 93° C x 2 minutes; 30 cycles of 93° C x 30 seconds, 56° C x 30 seconds, 72° C x 2 minutes; 72° C x 10 minutes. The product was analyzed on a 1.25% agarose gel to confirm size. A phenol-chloroform extraction was performed on the PCR amplicon as previously described. The *foxq1b-myc* open reading frame amplicon and the pBS_*foxq1b*P vector were digested with *Not*I HF and *Sac*I (NEB Cat. R0156S), as previously described. Restriction enzymes were inactivated by incubating digests at 65° C for 20 minutes. Vector linearization was confirmed on a 1% agarose gel. The digested pBS_*foxq1b*P vector and *foxq1b-myc* open reading frame amplicon were ligated and transformed as previously described. Single colonies were cultured in 15ml culture tubes containing 2ml LB and 100µg/ml Ampicillin, and incubated for 16 hours at 37° C and 250 rpm. Mini preps using the QIAGEN mini kit were performed on bacterial cultures in order to isolate the plasmid DNA, which was digested using *Not*I HF and *Sac*I, as described previously, and analyzed on a 1% agarose gel to confirm that the ligation reaction succeeded. A 500ml culture of a clone with the correct insert was processed using the QIAGEN maxi prep kit protocol and a glycerol stock was made, as described previously. The DNA (referred

to as pBS_*foxq1b*P_*foxq1b-myc*) was sequenced by the GSL to confirm the myc-tagged *foxq1b* open reading frame sequence.

Engineering and cloning of foxq1b polyA signal sequence

Forward (zf_foxq1b_*SacI*_polyAsignal_L) and reverse (zf_foxq1b_*Sac*I_polyAsignal_R) primers were designed to amplify the 600bp *foxq1b* polyA signal region flanked by *Sac*I restriction enzyme sites. A PCR was performed on the fosmid DNA using the PCR and thermal cycle conditions previously stated. Correct product size was confirmed on a 1% agarose gel. A phenol-chloroform extraction was performed on the PCR product, as previously described. The *foxq1b* polyA signal DNA amplicon and pBS_*foxq1b*P_*foxq1b-myc* vector were digested using *Sac*I, for 2 hours at 37^{o} C. Linearization of the vector was confirmed on a 1% agarose gel. An unexpected extra fragment was produced, and further analysis revealed that there was an additional *Sac*I site located in the center of the polyA signal sequence. A PCR was performed on the fosmid DNA using HotMaster Buffer and Taq Polymerase (5 Prime Cat. 2200300). PCR and thermal cycling condition used were previously described. The amplicon was cloned into the TOPO TA vector (Invitrogen Cat. K4575J10) using 4 µl of amplicon, 1 µl of TOPO vector, and 1µl salt solution and incubating at room temperature for 10 minutes. Transformation was performed using 50µl C2566 cells (NEB Cat. 2566I) following previously stated protocol. 50µl of the transformation solution was streaked on pre-warmed agar plates supplemented with 100µg/ml Ampicillin and incubated at 37^{o} C for 20 hours. Single colonies were cultured in 15ml culture tubes containing 3ml LB and 100µg/ml Ampicillin and incubated for 16

hours at 37º C and 250 rpm. Mini preps were performed following the QIAGEN mini kit to isolate the plasmid DNA from the cultures. The mini prep DNA was digested with *Sac*I at 37º C for 3 hours. A 1% agarose gel identified mini preps that contained the TOPO vector and *foxq1b* polyA signal insert, and GSL confirmed proper DNA sequence.

Mutagenesis was performed in order to remove the internal *Sac*I site. Forward (zf_foxq1b_polyAsignal_mut_L) and reverse (zf_foxq1b_polyAsignal_mut_R) primers were designed to change the first guanine in the *Sac*I sequence to a thymine. Mutagenesis was performed utilizing the QuikChange II XL Site-Directed Mutagenesis Kit (Agilent Technologies Cat. 200523) using 26ng of TOPO/polyA signal DNA, and 125ng of the forward and reverse primers. The PCR conditions, *Dpn*I restriction digest, and transformation of XL10-Gold Ultracompetent cells were carried out following the kit protocol. Cultures were made containing single colonies of bacteria, 2ml LB, and 100µg/ml Ampicillin, and incubated for 20 hours at 37º C and 250 rpm. Plasmid DNA was isolated by mini prep using the QIAGEN kit. The mini preps were digested using *Sac*I, and incubated in a 37º C water bath for 3 hours. Successful mutagenesis was visualized on a 1% agarose gel and confirmed by DNA sequencing.

The mutagenized clone was digested using 13.3µl 10X CutSmart Buffer, 3.3µl *Sac*I restriction enzyme, 30µl mini prep DNA, and 53.2µl water. A phenol-chloroform extraction was performed following previous protocol, and the linearized DNA was run on a 0.8% agarose gel. Linearized pBS_*foxq1b*P_*foxq1b-myc* was dephosphorylated with 4µl 10X Antarctic Phosphatase Reaction Buffer and 1µl Antarctic Phosphatase (NEB Cat. M0289S)

for 1 hour at 37° C and 5 minute at 70° C, in order to prevent self re-ligation. Ligation was performed using the dephosphorylated pBS_*foxq1b*P_*foxq1b-myc* and the *foxq1b* polyA signal insert. A transformation was carried out from the ligation reaction following the protocol previously described. Single colonies were cultured in culture tubes containing 2ml LB and 100µg/ml Ampicillin. Mini preps were performed on the bacterial cultures to isolate the plasmid DNA using the QIAGEN kit. The mini preps were digested using *Sac*I, and incubated for 16 hours at 37° C. A 1% gel was made to confirm polyA insertion into the vector, and renamed pBS_*foxq1b*P_*foxq1b-myc*_polyA.

Since the polyA fragment could ligate in either orientation, a PCR strategy was designed to distinguish the correct orientations. Briefly, forward (zf_foxq1b_ORFmyc_L) and reverse (zf_foxq1b_polyA_R) primers were designed, in which the forward primer resided in the *foxq1b* open reading frame and the reverse primer resided in the polyA signal. A PCR reaction on mini prepped pBS_*foxq1b*P_*foxq1b-myc*_polyA DNA was performed using thermal cycler conditions as previously described. GSL confirmed correct sequence of pBS_*foxq1b*P_*foxq1b-myc*_polyA. One clone with the correct insert was selected and scaled up by inoculating 500ml of LB supplemented with Ampicillin. The culturing and glycerol stock were performed as previously described. A restriction digest was performed on maxi prepped DNA using *Sca*I (NEB Cat. R3122S) to confirm that the vector contained the entire cassette consisting of *foxq1b* promoter, *foxq1b* ORF, myc-tag, and polyA signal, based on the presence of an 8kb and a 1.5kb fragment. After a 3 hour incubation at 37° C the digest was run out on a 1% agarose gel for confirmation.

Injection of foxq1b myc-tag construct

An I-*Sce*I (NEB Cat. R0694S) restriction digest was performed using pBS_*foxq1b*P_*foxq1b-myc*_polyA DNA at 37^{o} C for 1 hour to liberate the targeting cassette from the remainder of the cloning vector. 1µl 1% phenol red (SIGMA P5530) was added to 10µl of the restriction digest, and 1.5µl of the injection mixture was loaded into a needle made from borosilicate glass capillaries (Sutter Instrument, Item #:BF120-94-10, Lot: 161356-3), which were pulled on a Sutter Instrument Flaming/Brown micropipette puller (Model P-87) with the following settings: P= 400, T= 605, pull= 45, velocity= 110, and time= 195. The tip of the needle was clipped with forceps so that 1.5nl of DNA was injected into the 1-cell stage of wild type (Wik x Wik) zebrafish embryos. Injected embryos were placed in a Petri dish containing 0.5X E2 Medium (1L of 0.5X E2 Medium includes 7.5ml NaCl (1000mM), 0.5ml KCl (500mM), 0.5ml $MgSO_4$ (1000mM), 0.075ml KH_2PO_4 (1000mM), 0.05ml Na_2HPO_4 (500mM), 1ml $CaCl_2$ (500mM), 0.35ml Na_2HCO_3 (1000mM), 990.025ml autoclaved H_2O, and 0.5ml of 0.1% methylene blue) and incubated at 28^{o} C. At 24 hpf (hours post fertilization) embryos were bleached in a 250ml beaker filled with 170ml autoclaved water and 100µl of 5.25% sodium hypochlorite for 2 minutes with swirling. The bleach solution was removed and embryos were rinsed twice in sterile water for 5 minutes per rinse. Embryos were then transferred to sterile 0.5X E2 Medium. At 5 days post-fertilization, larvae were returned the fish room and reared to adulthood.

Foxq1b myc-tag potential founders

At three months, potential founders were genotyped. First, DNA was extracted from fin clips. Briefly, fish were anesthetized in individual cups filled with water and 500µl of buffered Tricaine (Western Chemical Inc. Cat. 200-226; 4mg/ml). A corner of the caudal fin of each zebrafish was sliced with a razor blade and placed in a PCR tube containing lysis buffer (2.5µl 10X Hot Master Buffer, 1.25µl 10mg/ml proteinase K (SIGMA Cat. P2308), and 21.25µl water). The fish was placed back in fresh water to recover. DNA was extracted from the fin clippings by vortexing, briefly centrifuging, and incubating the tubes at 55° C for 1 hour, followed by re-vortexing and centrifuging, and placing them back in the thermal cycler at 55° C for 30 minutes and 95° C for 15 minutes. PCR was performed as previously described, with HotMaster Buffer and Taq Polymerase using zf_foxq1b_ORFmyc_L (10µM stock) and 1µl zf_foxq1b_polyA_R (10µM stock) primers. The thermal cycler conditions used: 95° C x 45 seconds; 30 cycles at 95° C x 30 seconds, 55° C x 30 seconds, 72° C x 1 minute; 72° C x 10 minutes. PCR product was analyzed on a 2.5% agarose gel, wherein a 100bp would identify the endogenous *foxq1b* allele and a 150bp band would identify the *foxq1b-myc*.

Inheritance of myc-tag foxq1b DNA

Potential founders identified as described above were spawned with wildtype zebrafish. Pools of 15 embryos (48 hpf) were used for DNA extraction using 100µl NTES Mod2 (10mM Tris pH 8.0, 25mM EDTA, 50mM NaCl, and 0.5% SDS) per pool, supplemented with 1µl Proteinase K (10mg/ml) and incubated at 55° C with continuous

rocking until embryos dissolved (~1 hour). A phenol-chloroform extraction was performed following previous protocol. The pellets were resuspended in 70µl 1X TE buffer. PCR was conducted on extracted DNA using a forward primer (zf_foxq1b_ORFmyc_L) designed within the open reading frame of *foxq1b* and a reverse primer (zf_foxq1b_polyA1_R) designed within the polyA signal. As a control, β-actin was amplified using Zf-BactinF and Zf-BactinR primers (10µM stock). Amplicons were analyzed on a 2.5% agarose gel to determine if the embryos inherited the myc-tag *foxq1b* construct. A 100bp band represented endogenous *foxq1b*, and a 150bp band represented myc-tag *foxq1b* if present.

Expression of myc-tag foxq1b RNA in founder offspring

Forward and reverse primers were designed to span a 212bp fragment of *foxq1b*, in which the forward primer (zf_foxq1b_ORF1_L) annealed within the *foxq1b* open reading frame and the reverse primer (zf_foxq1b_myc_R) annealed within the myc-tag sequence. A myc-tag *foxq1b* founder, Tg(*foxq1b*:foxq1b-myc), was spawned with a wildtype (Wik x Wik) zebrafish, and RNA was extracted using TRI Reagent Solution (Ambion Cat. AM9738) from a pool of 90 embryos (30 hpf) in a 1.5ml tube. As a negative control, RNA was extracted from similarly staged wildtype embryos. The RNA pellet was resuspended in 40µl water, DNase treated using 5µl 10X DNase I Buffer (RNase-free), 1µl DNase I (Ambion Cat. AM2222), 8µl RNA (1257.4ng/µl), and 36µl water. The digest was mixed gently and incubated at 37^{o} C for 30 minutes. The digest was extracted with phenol-chloroform by adding 50µl of buffer-saturated phenol-chloroform and vortexing for 1 minute, followed by centrifuging at 14K rpm for 5 minutes. The aqueous phase was pipetted into a clean tube, and

5µl of 3M Sodium Acetate (pH 5.0) was added. The solution was vortexed and 125µl of 100% Ethanol was added. The tube was vortexed and placed at -20° C for 45 minutes. Afterwards, the tube was placed in a 4° C centrifuge and centrifuged at 14K rpm for 10 minutes. The supernatant was removed, 500µl of 70% Ethanol was added to the pellet, and the tube was re-centrifuged at 14K rpm for 5 minutes at 4° C. The pellet was dried and resuspended in 15µl water. cDNA was made by adding 2µl Oligo d(T) (IDT; 50µM), 2.8µl DNase I treated RNA (720.8ng/µl), and 7.2µl water in a PCR tube. The tube was placed in the thermal cycler at 80° C for 3 minutes, followed by the addition of 2µl 10X M MMLV Reverse Transcriptase (RT) Buffer, 1µl dNTPs (10mM stock), 0.25µl RNase Inhibitor Murine (NEB Cat. M0314S), 0.50µl M-MuLV Reverse Transcriptase (RT; NEB Cat. M0253S), and 4.25µl water. The contents were gently mixed and placed in the thermal cycler at 42° C for 1 hour, followed by a 10-minute incubation at 92° C. The RT reactions were supplemented with 40µl, and 2µl were used for PCR following the PCR and thermal cycler conditions described in the *Foxq1b myc-tag potential founders* section, but using 40 cycles instead of 30. A 2.5% agarose gel was made to confirm the presence of *foxq1b-myc* RNA.

Immunohistochemistry of myc-tag foxq1b protein in founder offspring

The Tg(*foxq1b*:foxq1b-myc) founders were spawned with wildtype (Wik x Wik) zebrafish. The embryos were place in 10ml of E2 medium supplemented with 2µl of 1µM 1-phenyl 2-thiourea (PTU) (SIGMA Cat. P7629) at 24 hpf, to prevent pigmentation. At 48 hpf the embryos were dechorionated and placed in 1ml of 4% Paraformaldehyde (PFA) (Electron Microscopy Sciences Cat. 19208) for fixation. Embryos were rocked at room temperature for

4 hours, and then rinsed in 1ml of 1X PBST (Phosphate Buffered Saline (Fisher Scientific Cat. BP665-1), 0.1% Tween-20 (Fisher Scientific Cat. 9005-64-5)) at room temperature. The PBST was removed and the embryos were washed twice with methanol, after which they were stored at -20^{o} C in 1ml of fresh methanol. The embryos were serially rehydrated in 95% MeOH + 5% PBST, 75% MeOH + 25% PBST, 50% MeOH + 50% PBST, and 25% MeOH + 75% PBST, followed by washing four times in 1ml PBST for 5 minutes. Embryos were permeabilized by adding 1ml of ice-cold acetone (Fisher Scientific Cat. 67-64-1) and incubating for 8 minutes at -20^{o} C. The embryos were again washed four times in 1ml PBST for 5 minutes and blocked in 1ml block (PBST + 5% Sheep Serum (SIGMA Cat. S3772)) by rocking for 1 hour at room temperature. Anti-myc primary antibody (Invitrogen, Cat. 46-0603) was placed on the embryos at a 1:100 dilution in block, and rocked at 4^{o} C overnight. The next day, the antibody was removed and embryos were washed five times at room temperature in 1ml block for 10 minutes per wash, followed by three washes in 1ml PBST for 10 minutes. A 1:1000 dilution of Alexa Fluor 594 donkey anti-mouse secondary (Invitrogen, Cat. A-21203, Lot: 491315) in block was applied to the embryos. The tubes were wrapped in aluminum foil, and rocked at 4^{o} C overnight. The embryos were washed five times in 1ml block for 10 minutes, then three times in 1ml PBST for 10 minutes. DAPI (4',6-diamidino-2-phenlindole; Life Technologies Cat. D1306) was applied for 20 minutes at room temperature and at a 1:500 dilution from a 14.3mM stock to counter-stain nuclei. The DAPI was removed and replaced with 1ml block. The embryos were placed on glass bottom dishes (MakTek, Cat. P35G-0-10-C) and mounted in 1% low melt agarose. The plates were flooded

with1X PBS once the agarose solidified. Imaging was performed using confocal microscopy on a Zeiss LSM-720 located at North Carolina State University Cellular and Molecular Imaging Facility.

AhR regulation of foxq1b-myc

DMSO or 3nM TCDD was exposed to 6 hpf *foxq1b-myc* embryos for 24 hours. RNA was extracted from *foxq1b-myc* embryos (4 replicates of 15 pooled embryos) at 48 hpf, quantified using the Agilent Bioanalyzer, normalized, and reverse transcribed to make cDNA. qPCR analysis was performed using GAPDH left and GAPDH right primers for normalization, cyp1a1_L and cyp1a1_R primers for amplification of *cyp1a* (a known AhR target), zf_foxq1b_qpcrL2 and zf_foxq1b_qpcrR2 primers for amplification of *foxq1b* (both endogenous and *foxq1b-myc*), and zf_foxq1b_ORF1_L and zf_foxq1b_myc _R primers for the amplification of *foxq1b-myc*. The qPCR reaction included 5.125µl water, 12.5µl 2X Brilliant II SYBR Green QPCR Master Mix, 0.375µl ROX (1:500), 1µl forward primer (10µM stock), 1µl reverse primer (10µM stock), and 5µl cDNA. A Comparative Quantitation (Calibrator) qPCR experiment using MxPro software was performed using the following thermal parameters: 95^{o} C x 10 minutes; 50 cycles of 95^{o} C x 30 seconds, 55^{o} C x 30 seconds, 72^{o} C x 30 seconds; 95^{o} C x 30 seconds; 55^{o} C x 30 seconds; 95^{o} C x 30 seconds. The log fold change of *cyp1a1*, endogenous *foxq1b*, and *foxq1b-myc* genes when exposed to 3nM TCDD was compared to the DMSO replicates (calibrators).

Table 3: Primer names and sequences used to create *foxq1b-myc* construct. List of all the primer names and sequences that are mentioned in the methods section. *Bold and underlined nucleotides are the nucleotides mutated through mutagenesis.

Primer Name	Sequence (5 '- 3')
zf_foxq1b_*Kpn* I_Prom_L	AAGGTACCTAAATTGATGCTGGTGGTCTATTTC
zf_foxq1b_*Not* I_3UTR_R	AAGCGGCCGCTGGCAGAGCTTCAGAAAGTTCGAAG
M13F	GTAAAACGACGGCCAG
zf_foxq1b_prom_L2	TGTGTCTGATCAGCAACTTGAAA
zf_foxq1b_prom_L3	CCAACGACCTTCTTGCTGTC
zf_foxq1b_prom_L4	AGCTTGTTCAGGTGTGTTTGA
zf_foxq1b_prom_L4.2	AGCCACTGATGCTACGACAT
zf_foxq1b_prom_L5	TGTTCACTCCACATAAGTTTGC
zf_foxq1b_prom_L5.2	GCTTGCATAACAGAAAGAGTCG
zf_foxq1b_prom_L6	ACCACCCAGCATTCTTTAGAGT
zf_foxq1b_prom_L7	ACATATGTCACGTCATGCACA
zf_foxq1b_prom_L7.2	TCAGGTTTCCTCCACAGTCC
zf_foxq1b_prom_L7.3	ACCTTGTAATGAACTGCTAGTCA
zf_foxq1b_qL1	ATGATCCCGGTGTTTTTGTG
M13R	CAGGAAACAGCTATGAC
zf_foxq1b_*Not* I_m-2ORF_L	AAGCGGCCGCCATGAAACTGGAGGTTTTCTGCGGGA
zf_foxq1b_*Sac* I_m-2ORFmyc_R	AAGAGCTCTTACAGGTCCTCCTCTGAGATCAGCTTCTGCTCCGACAACAAATAGTCAATTTTGAAC
zf_foxq1b_*Sac* I_polyAsignal_L	AAGAGCTCCATTGGGTACTTTGTGATGGGGAAC
zf_foxq1b_*Sac* I_polyAsignal_R	AAGAGCTCAACTGGTTGAAAATGAGCATGCAAT
zf_foxq1b_polyAsignal_mut_L	TGAACTATATGAGAGGC**T**AGCTCAGTTTGTGAGGCTCCTG
zf_foxq1b_polyAsignal_mut_R	CAGGAGCCTCACAAACTGAGCT**A**GCCTCTCATATAGTTCA
zf_foxq1b_ORFmyc_L	CTCTCAATCCCGCATACGA
zf_foxq1b_polyA_R	CGAAGTTCCCCATCACAAAG
zf_foxq1b_polyA1_R	TTCCCCATCACAAAGTACCC
Zf-BactinF	CGAGCAGGAGATGGGAACC
Zf-BactinR	CAACGGAAACGCTCATTGC
zf_foxq1b_ORF1_L	ACACTGTGCTGCCGTATGTC
zf_foxq1b_myc_R	ATCAGCTTCTGCTCCGACAA

Table 3 Continued

Primer Name	Sequence (5' - 3')
Gapdh left	TGGGCCCATGAAAGGAAT
Gapdh right	ACCAGCGTCAAAGATGGATG
zf_cyp1a1_L	GGATATCAACGAACGCTTCA
zf_cyp1a1_R	TTCTCATCGGACACTTGCAG
zf_foxq1b_qpcrL2	ATCCTCAGTCGACCCTTCAG
zf_foxq1b_qpcrR2	CAGCTGGAATGCGAAAAAGT
zf_foxq1b_ORF1_L	ACACTGTGCTGCCGTATGTC
zf_foxq1b_myc_R	ATCAGCTTCTGCTCCGACAA

Results

A 6.7 kb fragment of the locus encoding the zebrafish transcription factor, *foxq1b* (Chr. 2) consisting of the complete ORF, polyA signal, and 5.2kb directly upstream of the transcription start site, was successfully cloned into the multiple cloning site (MCS) of pBluescriptII/SK+. A myc-tag was engineered in frame with the 3'end of the ORF, directly before the stop codon (Figure 1) to facilitate downstream applications, including immunohistochemistry and ChIP-seq analysis. Intermediate steps of the cloning strategy are summarized in Figure 2.

The pBluescriptII/SK+ plasmid was previously modified to contain two I-*Sce*I meganuclease restriction enzyme sites flanking the MCS (kind gift from Dr. Jochen Wittbrodt, Heidelberg). The purpose of these sites is to allow excision of the cassette – in this case the engineered *foxq1b-myc* gene – from the vector before injecting the construct into embryos. Meganuclease restriction sites are not found in zebrafish; therefore, the digest can be injected directly into the embryo without the need to inactivate the I-*Sce*I enzyme. 1.5nl of the digest was injected into 500, 1-cell stage, wild-type zebrafish embryos. The fish were reared to adulthood and genotyped via fin clip to verify that the cassette had been integrated in the genome (Figure 3). The primer strategy in Figure 3A was utilized to identify 9 potential founders that harbored the transgene, representing about an 18% success rate since many of the injected embryos did not survive till adulthood.

Potential founders were crossed to wild-type zebrafish and 15 of their embryos were pooled for DNA extraction. The primer strategy used in Figure 3A was utilized to amplify

endogenous *foxq1b* and *foxq1b-myc* in the offspring. Of the nine potential founders only one, a female, transmitted the transgene to its offspring (Figure 4). The F1 embryos from this founder were reared to adulthood.

In order to confirm that the transgene-positive F1 embryos expressed the transgene, 90 embryos were pooled for RNA extraction and reverse transcribed. A forward primer was designed within the *foxq1b* open reading frame and a reverse primer designed within the myc sequence to validate transcription of the transgene (Figure 5).

Translation of the transgene mRNA was assessed in 48 hpf embryos by immunohistochemistry, using a mouse anti-myc monoclonal primary antibody detected by a donkey anti-mouse secondary antibody labeled with Alexa Fluor 594. DAPI was used to counter-stain nuclei. Since foxq1b is a transcription factor and presumably located within the nucleus, DAPI enabled us to visualize nuclei and ascertain if foxq1b localized to the nucleus (Figure 6). The embryos were imaged at 40X magnification by confocal microscopy. We observed that foxq1b-myc indeed localized to several nuclei near the otic vesicle and within the jaw region (Figure 6).

Since AhR is a known activator of *foxq1b* transcription, it was hypothesized that *foxq1b-myc* embryos exposed to the AhR ligand TCDD would cause an upregulation of the *foxq1b-myc* transgene. Tg(*foxq1b:*foxq1b-myc) embryos were exposed to DMSO or 3nM TCDD at 6 hpf for 24 hours. At 48 hpf RNA was isolated from the embryos and reverse transcribed to make cDNA. Quantitative PCR was utilized to quantify the expression levels of endogenous *foxq1b, foxq1b-myc, cyp1a,* and *gapdh* . *Gapdh* was used as a normalizer,

while a known downstream target of the AhR, *cyp1a*, was used as a positive control. Endogenous *foxq1b* expression levels increased 4-fold when exposed to TCDD, whereas *foxq1b-myc* showed no significant change (Figure 7).

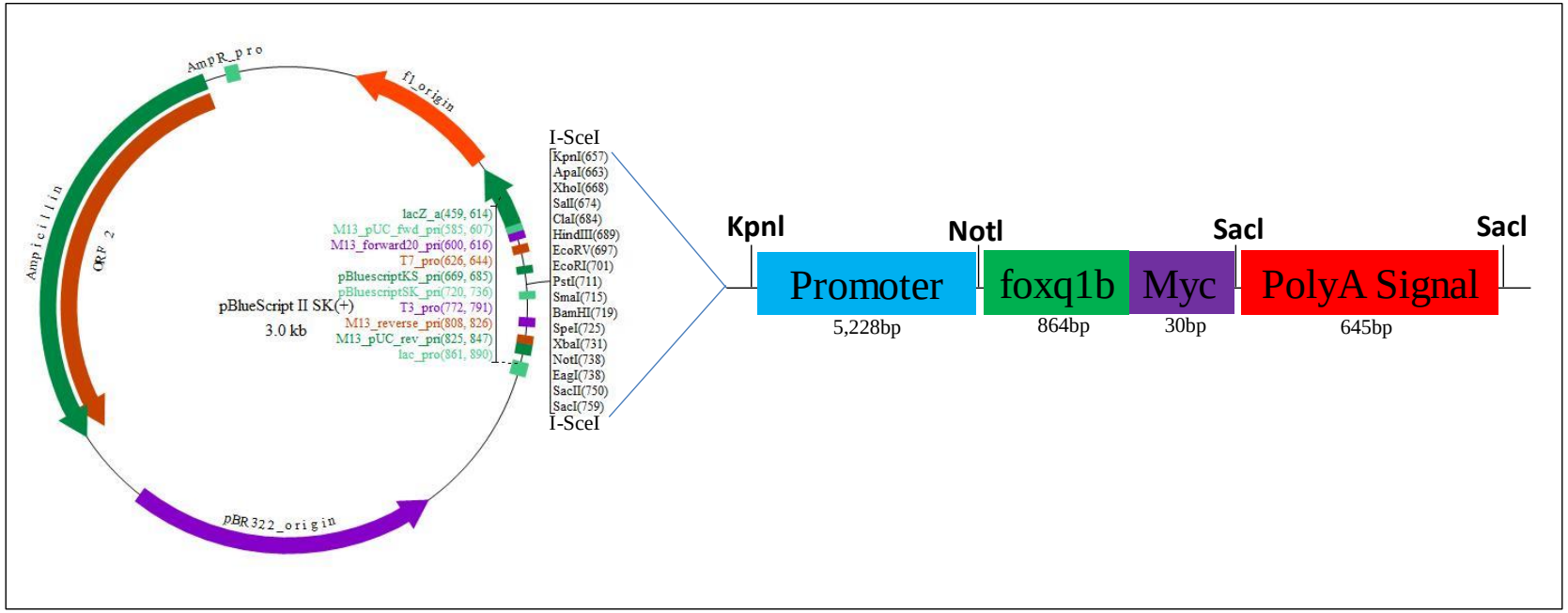

Figure 1: Cloning strategy of the *foxq1b-myc* construct in the pBluescriptII/SK+ plasmid. The cloning strategy is described in Materials and Methods.

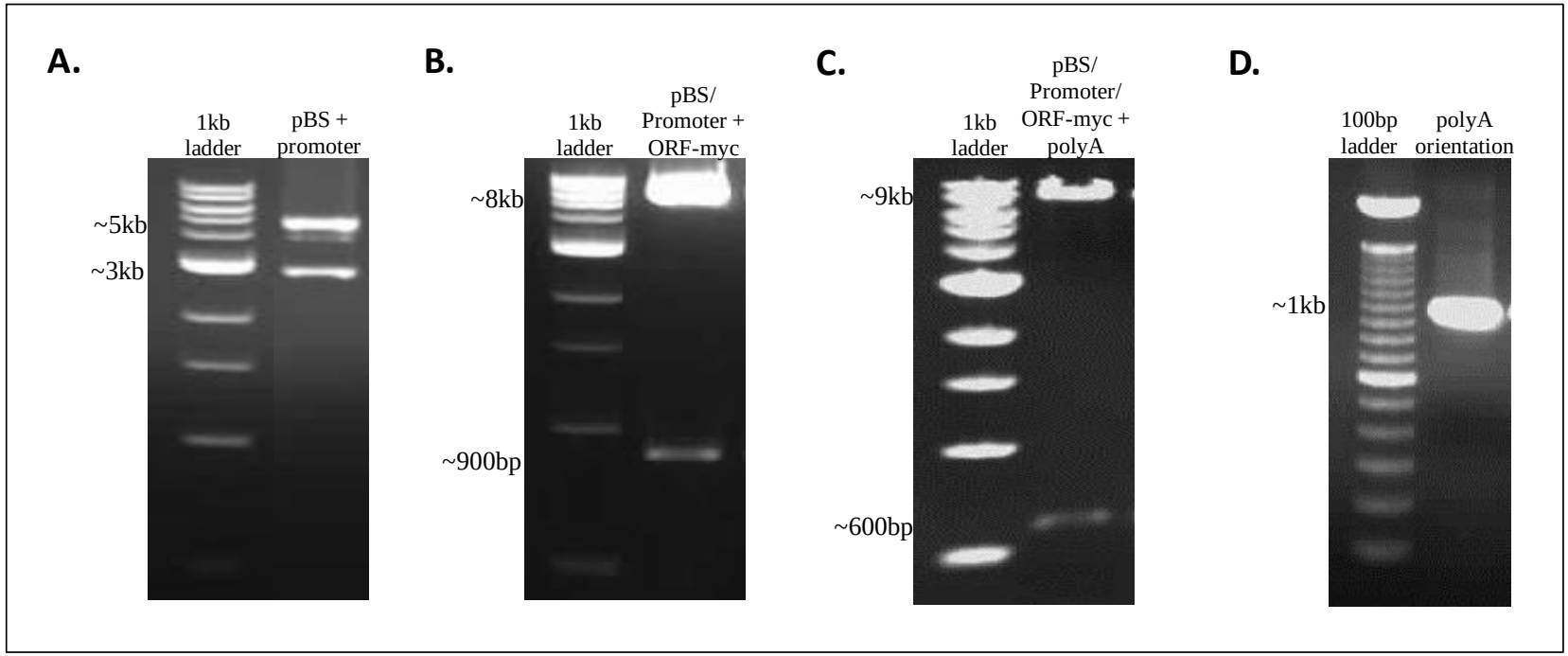

Figure 2: Intermediate steps in the cloning strategy as visualized by gel electrophoresis. A. Restriction digest with *Kpn*I and *Not*I confirms the insertion of the ~5kb *foxq1b* promoter into the ~3kb plasmid. **B.** Restriction digest with *Not*I and *Sac*I confirms the insertion of the ~900bp *foxq1b* open reading frame modified to carry a myc-tag into the ~3kb plasmid containing the ~5kb promoter (~8kb total). **C.** Restriction digest with *Sac*I confirms the insertion of the ~600bp *foxq1b* polyA signal into the ~3kb plasmid containing the ~5kb promoter and ~900bp open reading frame (~9kb total). **D.** PCR amplification using a forward primer that resides in the *foxq1b* open reading frame and a reverse primer that resides in the polyA signal confirmed proper polyA signal orientation due to the production of a 977bp fragment.

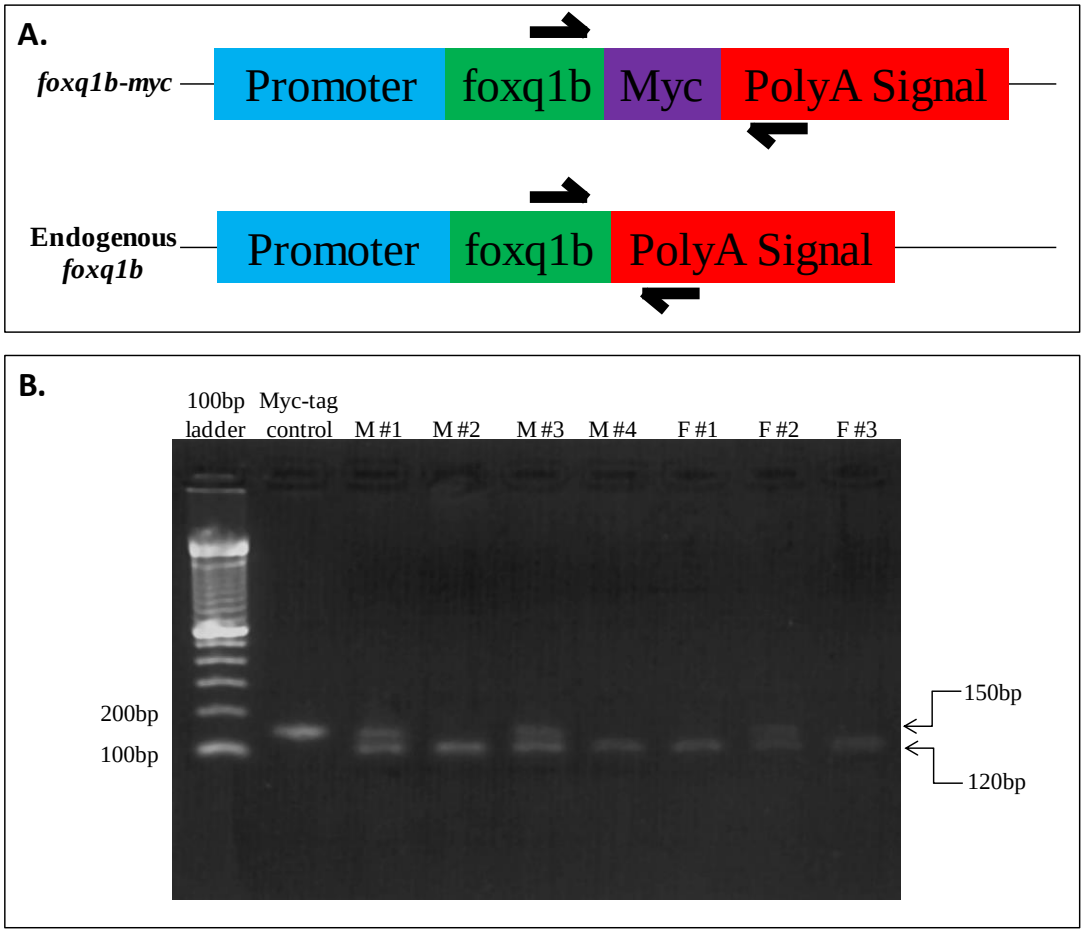

Figure 3: Identification of *foxq1b-myc* potential founders. A. Primer strategy: Forward primer was designed within the open reading frame of *foxq1b* and the reverse primer was designed within the polyA signal. The primers are designed to amplify a 150bp product from *foxq1b-myc* and a 120bp product from the endogenous locus. **B.** Genotypes are confirmed by gel electrophoresis PCR products derived from nine fish. The presence of two fragments represent potential founders containing both *foxq1b-myc* and endogenous *foxq1b*. Plasmid DNA containing *foxq1b-myc* (see Figure 1) was diluted and used as a positive control.

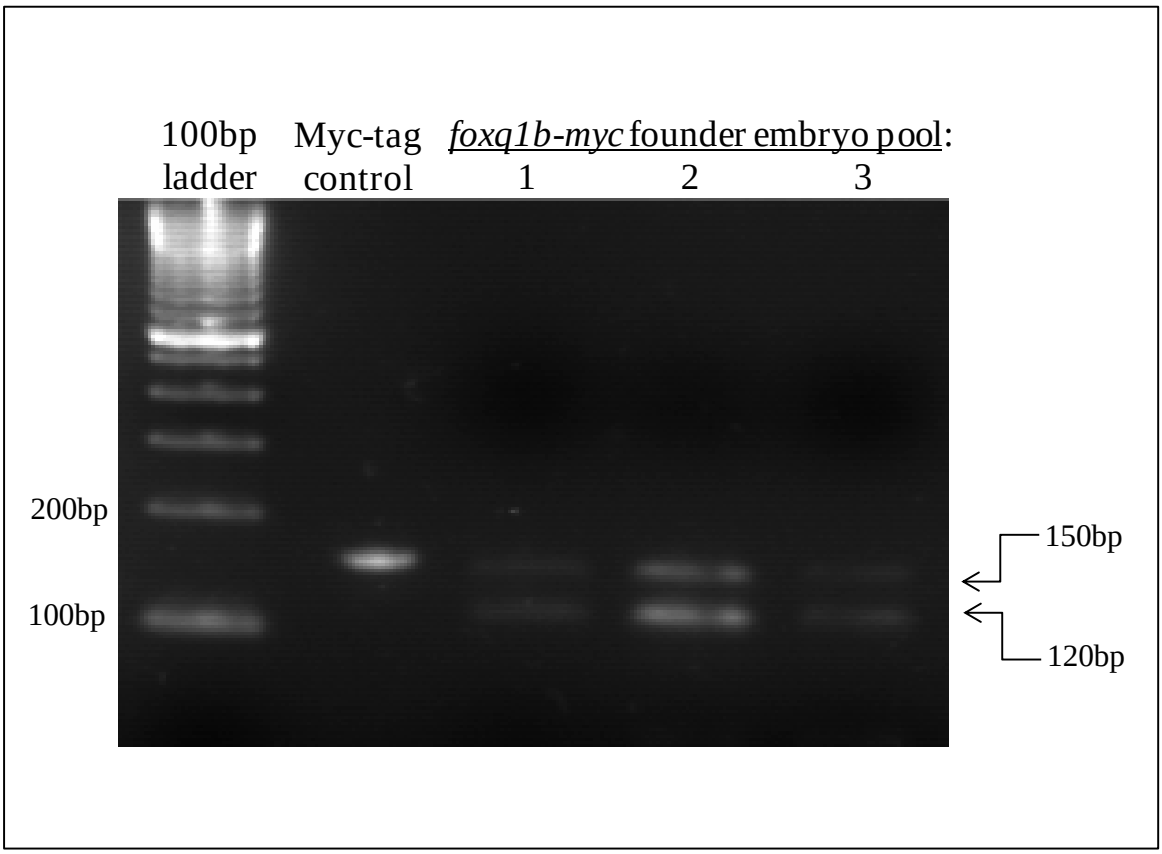

Figure 4: Transmission of *foxq1b-myc* to offspring by female founder #2. Embryos were pooled into three pools of 15 embryos each. Genomic DNA was extracted from each pool and used for PCR to confirm the transmission of the *foxq1b-myc* transgene from female #2. The strategy used to distinguish between the endogenous and transgenic loci is described in Figure 3B.

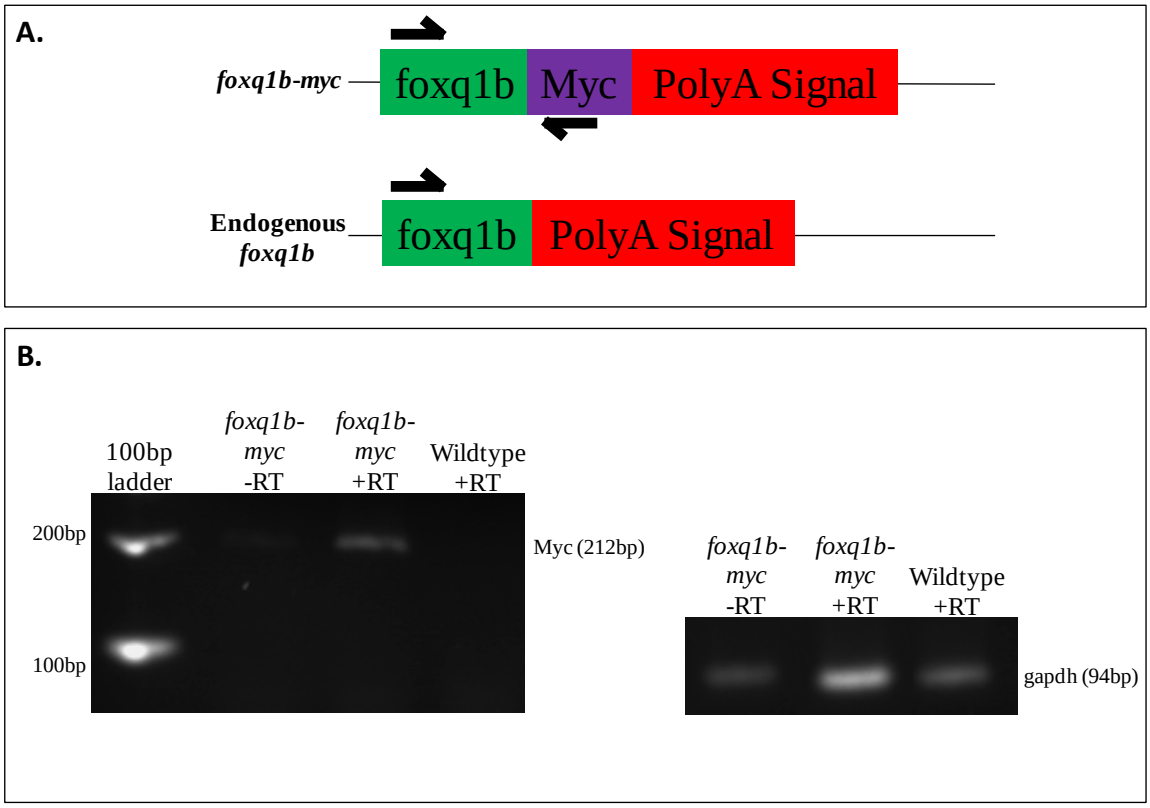

Figure 5: Transgene-positive offspring transcribe *foxq1b-myc* mRNA. A. Primer strategy: Forward primer was designed within the *foxq1b* open reading frame, reverse primer was designed within the myc-tag sequence. If the *foxq1b-myc* mRNA is present, a band at 212bp will be produced by RT-PCR. If the *foxq1b-myc* RNA is not present, no band will be produced. **B.** Gel electrophoresis of RT-PCR products. RNA was DNase-treated prior to reverse transcriptase reaction as described in Materials and Methods. –RT: no reverse transcriptase. +RT: reverse transcriptase; gapdh was used as a positive control.

Figure 6: Foxq1b-myc protein is nuclearly localized to cells in the periphery of the otic vesicle and jaw region. Immunohistochemistry was utilized as described in Materials and Methods to detect foxq1b-myc protein in 48 hpf embryos at 40X magnification using confocal microscopy. **A.** The red box indicates location of image B. The green box indicates location of image C. **B.** Left image is DAPI stain of the cell nuclei, right image is Alexa Fluor staining of the foxq1b-myc protein overlapping DAPI around the otic vesicle. **C.** Left image is DAPI stain of the cell nuclei, right image is Alexa Fluor staining of the foxq1b-myc protein overlapping DAPI in the ventral jaw. *The white boxes in B and C indicate the overlap of the myc-tag foxq1b protein with the cell nuclei.

A.

B.

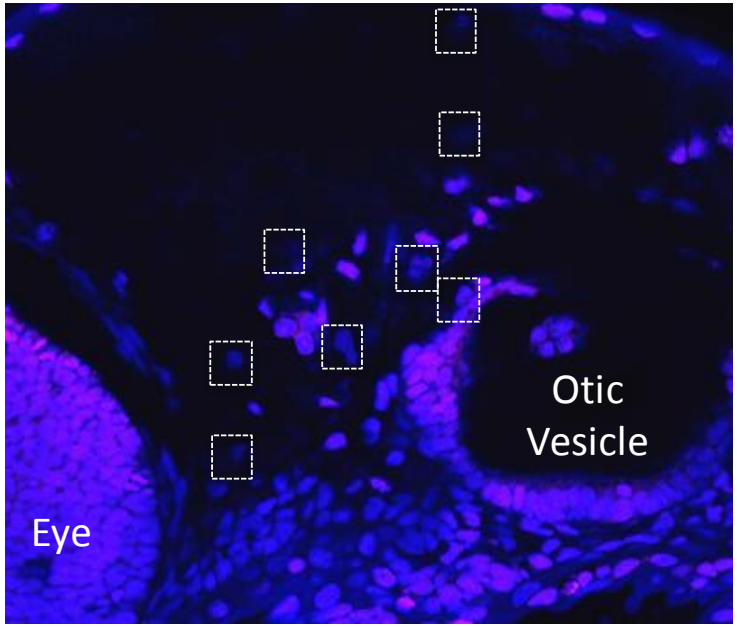

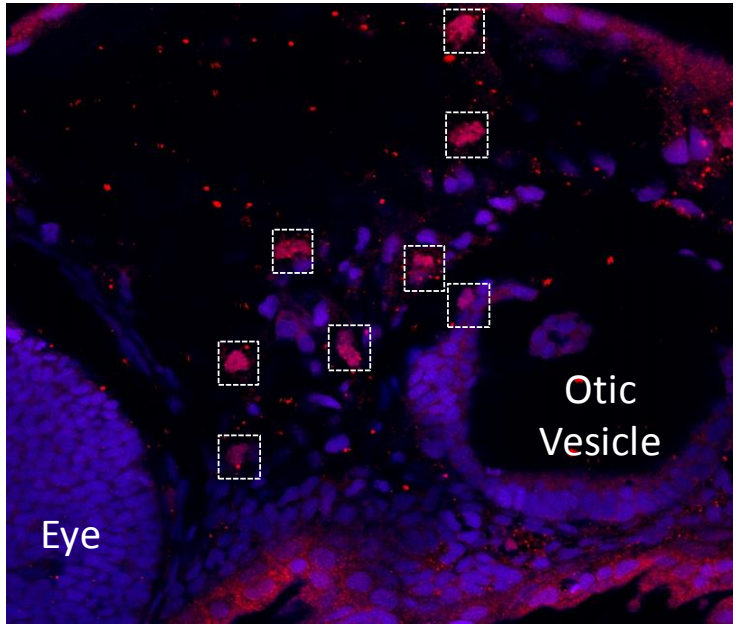

C.

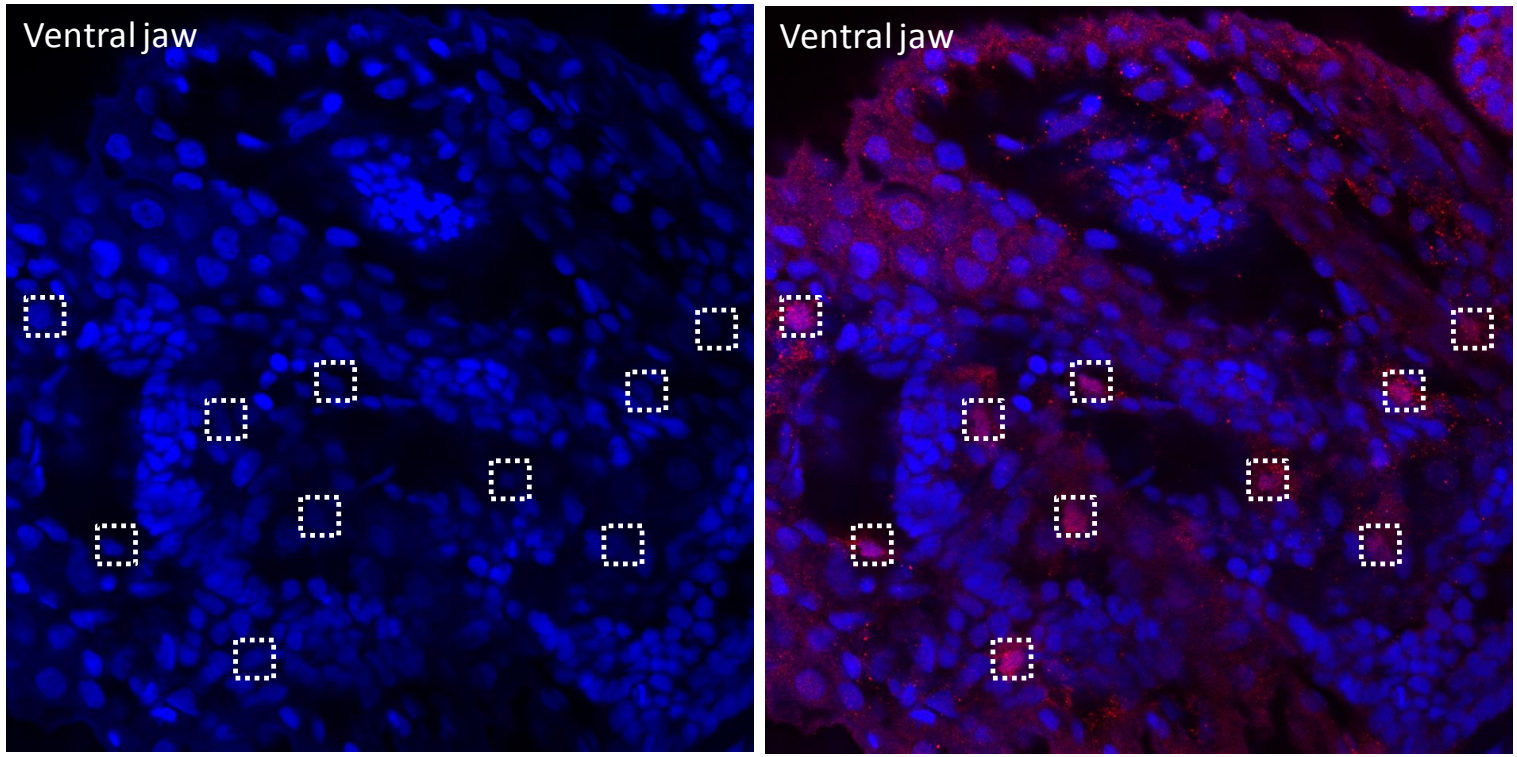

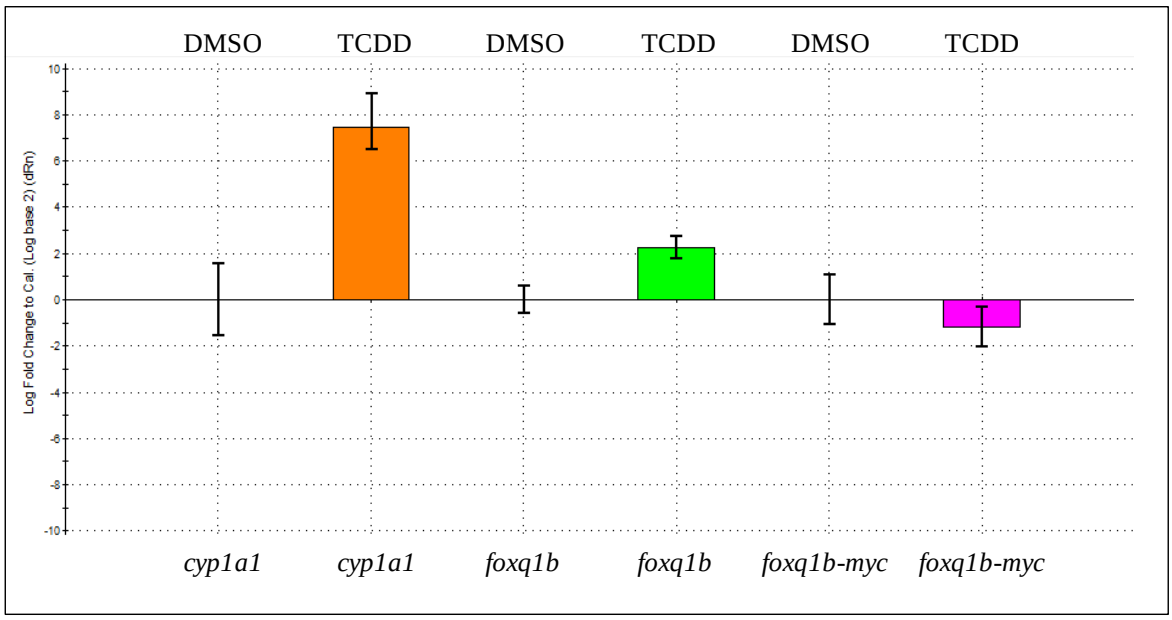

Figure 7: RT-qPCR of 48 hpf *foxq1b-myc* zebrafish exposed to DMSO or 3nM TCDD. Each bar represents the average of four biological replicates consisting of 15 embryos each. *Foxq1b* primers would amplify both the endogenous, as well as *foxq1b-myc*. *Foxq1b-myc* reverse primer included the myc-tag in order to only amplify the *foxq1b-myc* transgene. *Cyp1a1* was upregulated 128-fold, and endogenous *foxq1b* 4-fold, whereas *foxq1b-myc* showed no significant change.

Discussion

A whole genome duplication occurred in the evolutionary history of zebrafish, which most likely explains the existence of two paralogs of the *foxq1* transcription factor, namely *foxq1a* and *foxq1b.* The expression profile of mammalian *FOXQ1* and the effects caused by inactivating it (Goering 2008) are closely mirrored in zebrafish *foxq1b,* whereas this is not the case for *foxq1a*. In fact, *foxq1a* is maternally deposited and generates no phenotype when knocked down using morpholinos. In addition, its expression domain has been largely undetectable (A. Planchart, personal communication). Therefore, based on these observations, *foxq1b* has been the primary focus of our lab since it appears to be more functionally similar to the human *FOXQ1* gene.

An engineered allele of *foxq1b,* under the control of the *foxq1b* promoter, designed to encode a modified protein in which the C-terminus is tagged with the myc epitope, is hypothesized to be expressed in the same cells as the endogenous *foxq1b* gene. The myc-tag was engineered to not interfere with the function of foxq1b, since the C-terminal tail plays no known role in the binding and regulation of foxq1b. This engineered allele of *foxq1b* was successfully integrated into the zebrafish genome and intergenerationally transmitted from founder to offspring, in which it was transcribed, and translated. This transgenic line will be useful for further studies of the role *FOXQ1* plays in both embryonic development and cancer.

Since *foxq1b* encodes a transcription factor, determining the direct downstream targets of this protein will provide a greater understanding of the mechanisms involved in

development and cancer. Initial transcriptomic analysis of the *foxq1b* morphant yielded a list of genes that are potential downstream targets of foxq1b and play significant roles in both development and carcinogenesis; however, whether they are direct or indirect targets remains a subject of speculation. Thus, the foxq1b-myc transgenic line may prove valuable for further characterization of these genes, especially by chromatin immunoprecipitation sequencing (ChIP-seq). Using this procedure, genomic DNA cross-linked to foxq1b-myc protein can be isolated using anti-myc antibodies, reverse cross-linked and sequenced, thus helping to validate morpholino data by determining if foxq1b regulates these genes directly by binding to their promoter regions.

A common thread tying several genes within the morphant dataset is the observation that they play a role in apoptosis, which is necessary for proper embryonic development (Brill 1999). Disruption of this pathway can lead to abnormalities during development, as well as contribute to cancer formation and progression later in life, presumably because cells with mutations arising early in development are not eliminated but remain and cause havoc later in life. Determining if foxq1b directly binds and regulates these genes could provide greater evidence about its function in development and cancer.

Foxq1b expression has been shown to be upregulated through TCDD activation of AhR (Planchart and Mattingly 2010); however, TCDD exposure to Tg(*fox1b*:foxq1b-myc) embryos resulted in no change of expression. Since AhR regulates *foxq1b* by directly binding to its promoter, DREs located within the first 5kb upstream of the transcription start site are either not sufficient, not recognized by the AhR, or both. Therefore, the remaining three

DREs located upstream of the 5kb promoter region are candidates for mediating AhR regulation of *foxq1b*. Alternatively, it is possible that the integration site harboring the transgene, which is presumed to be different from the location of the endogenous gene, is impeding regulation of the transgene by ligand-activated AhR. Further studies will be required to ascertain the cause of this lack of regulation by AhR.

Conclusion

The downstream targets of *FOXQ1* that are directly regulated by the binding of this transcription factor are still unknown. The Tg(*foxq1b*:foxq1b-myc) zebrafish has created opportunities for learning more about the regulatory landscape of foxq1b, as well as understanding how this regulation is necessary for embryonic development. In addition, since FOXQ1 is aberrantly upregulated in human carcinoma, foxq1b-myc transgenic zebrafish may provide opportunities to study foxq1b's direct relationship with genes involved in cancer progression and provide insight into potential targets of cancer therapeutics.

III. *FOXQ1B* GENETIC KNOCKOUT UTILIZING CRISPR-CAS TECHNOLOGY

Abstract

Many genetic and environmental factors can lead to craniofacial birth defects, yet much is still unknown about the genetic mutations involved in craniofacial abnormalities. The zebrafish transcription factor, *foxq1b*, has been shown to play a significant role in cranial patterning. A knockdown of *foxq1b* by a morpholino causes significant jaw deformities in zebrafish. A full knockout of *foxq1b* using CRISPR-Cas technology will provide greater knowledge on the importance of *foxq1b* in development, as well as how it contributes to the craniofacial structure of an organism. This will provide useful information about a gene whose misregulation could potentially be involved in craniofacial anomalies.

Introduction

Craniofacial abnormalities are birth defects that result in aberrant development of the skull or facial features. Cleft lip and cleft palate are among the most widely known craniofacial abnormalities, which are seen in about 1 in 700 births (Vandera 1987), and require extensive surgery. Since the development of the head is so complex, many of the mechanisms and genes involved are still unknown (Francis-West 2003). Studying genes involved in craniofacial development, and the different mutations they might undergo, will ultimately lead to a better understanding of how and why craniofacial birth defects occur.

The forkhead box transcription factor *FOXQ1*is known to play a significant role in development, especially within the facial region. The knockout of *Foxq1* in mice has been shown to result in cranial abnormalities including diminished brain vesicles, shrinkage of the third and lateral brain ventricles, and a decrease in cerebrospinal fluid (Goering 2008). These

results demonstrate the importance of *Foxq1*'s involvement in proper craniofacial development.

Preliminary data on *foxq1b's* role in zebrafish development has also shown it is necessary for a proper craniofacial phenotype. *In situ* hybridization using a *foxq1b* probe reveals that *foxq1b* mRNA expression is primarily located within the cranial region of zebrafish (Figure 8). To determine *foxq1b*'s function within this region, a *foxq1b* morpholino was used to knockdown *foxq1b* expression in a *sox10*::egfp transgenic zebrafish line. The *sox10*::egfp line allows for egfp expression under the control of the *sox10* promoter. *Sox10* is a marker for neural crest cells, which is useful for illuminating cells responsible for craniofacial cartilage and bone development (Carney 2006). The *foxq1b* morphant resulted in significant craniofacial abnormalities, specifically in the jaw region when compared to the wild-type zebrafish (Figure 9), suggesting *foxq1b* might play a role in the patterning of the craniofacial skeleton. Knocking down *foxq1b* with a morpholino has shown that *foxq1b* is required for proper development; however, the hypothesis that *foxq1b* is necessary for survival is still unknown.

CRISPR (clustered regularly interspersed short palindromic repeats) is the adaptive immune system in bacteria that provides protection against viruses and foreign pathogens (Sternberg 2014). It consists of a CRISPR RNA (crRNA), a transacting RNA (tracrRNA), and a Cas9 endonuclease, which together target a specific DNA sequence and perform a double stranded break (Deltcheva 2011). Through non-homologous end joining, insertions and deletions in the targeted DNA sequence cause a loss of gene function (Jiang 2013).

Recently, this technology has been utilized to knockout specific genes in eukaryotic organisms (Sternberg 2014). A single guide-RNA (gRNA), which mimics the crRNA and tracrRNA, can be designed to scan the genome, and with the help of Cas9, locate and cut a region in the DNA that is of interest (Jinek 2012), and ultimately knock out the gene's function.

Utilizing the adaptive immune system in bacteria, CRISPR-Cas9 successfully mutagenized the *foxq1b* gene, and rearing these zebrafish to adulthood will allow for a full *foxq1b* knockout to be produced. This will be useful for observing phenotypic responses to a full knockout of *foxq1b*, as well as, determining the degree at which *foxq1b* expression is necessary for zebrafish survival.

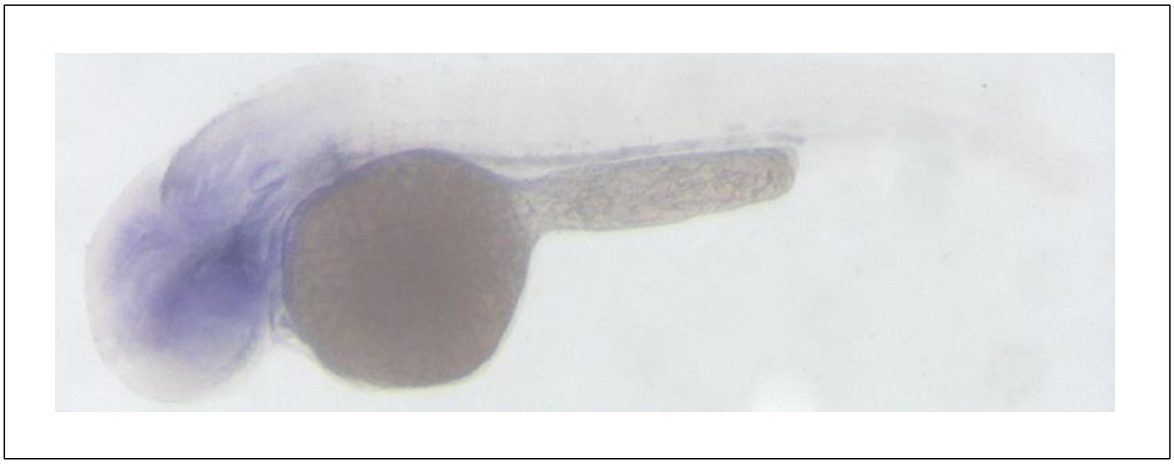

Figure 8: In situ hybridization using a foxq1b probe. *In situ* on a 48 hpf embryo shows *foxq1b* mRNA expression primarily within the craniofacial region of the zebrafish. Expression also extends along the gastrointestinal tract. (Preliminary research conducted by Planchart Lab).

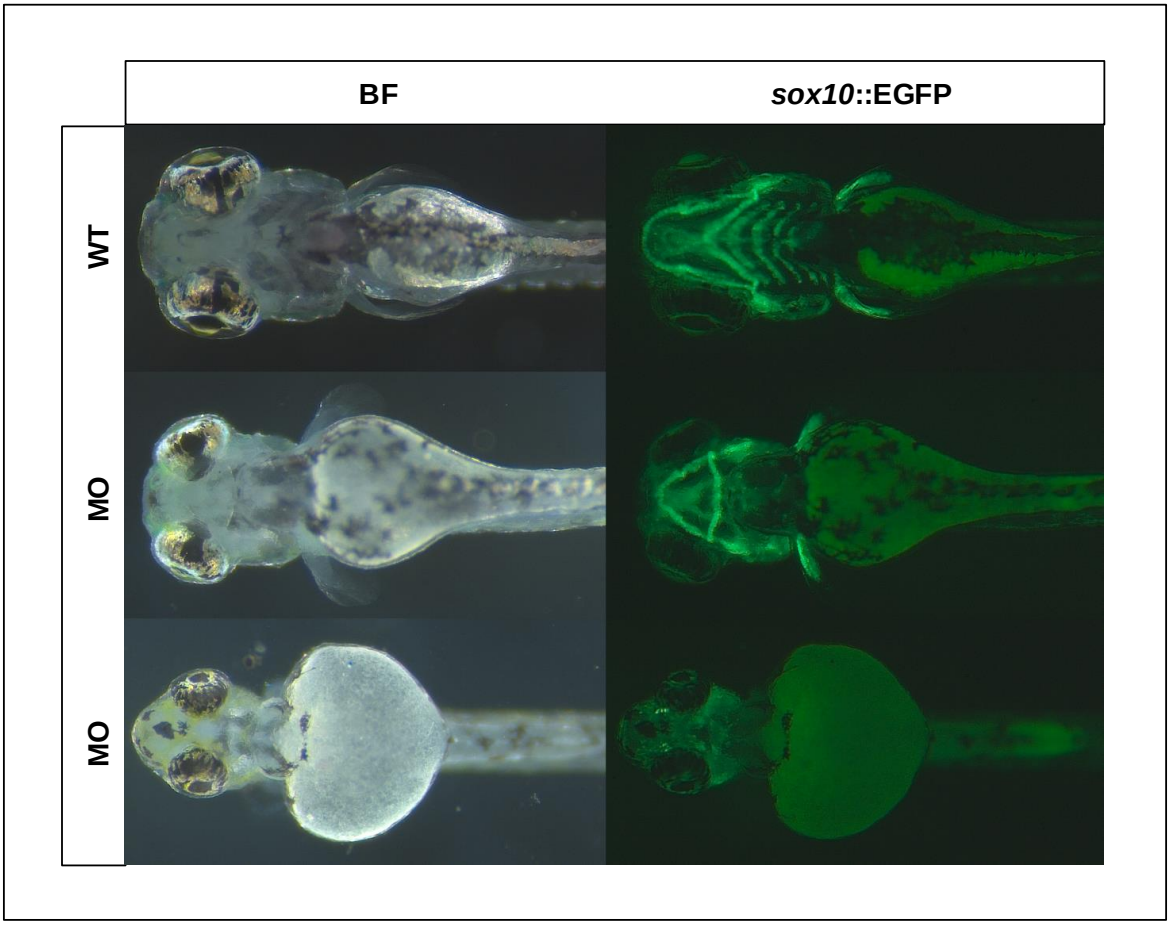

Figure 9: Knockdown of foxq1b expression using a morpholino. A *foxq1b* morpholino was injected in the one cell stage *sox10*::egfp zebrafish embryos. WT (wild-type) vs. MO (morpholino) injected embryos observed using BF (brightfield) and fluorescence microscopy. (Preliminary research conducted by Planchart Lab).

Materials and Methods

pT7-gRNA and pT3TS-nCas9n Plasmid DNA Isolation

A stab culture of pT7-gRNA (Addgene plasmid #:46759, Jao 2013) and pT3TS-nCas9n (Addgene plasmid #:46757, Jao 2013) were streaked on agar plates supplemented with 100µg/ml Ampicillin (Sigma Cat. A5354), and incubated for 20 hours at 37º C. Single colonies were cultured in 3ml LB and 100µg/ml Ampicillin at 37º C for 20 hours and 250 rpm. 100µl of the cultures were transferred to flasks containing 500ml LB and 100µg/ml Ampicillin, and incubated for 20 hours at 37º C and 250 rpm. Glycerol stocks were made as described previously. A maxi prep was performed on the remaining culture using the QIAGEN kit (Cat.12163) and protocol.

Restriction Digest of pT7-gRNA

The pT7-gRNA plasmid was linearized with *Bsm*BI, as follows: 4µl 10X NEB Buffer 3.1 (NEB Cat. B7203S), 1µl *Bsm*BI (10,000U/ml) (NEB Cat. R0580S), 1µl pT7-gRNA plasmid DNA (5.4µg/µl), and 24µl water were gently mixed and incubated for 3 hours at 37º C. The digest was resolved on a 1% agarose gel, and gel-extracted to isolate the 2500bp band following the QIAGEN QIAquick Gel Extraction kit (Cat. 28704) and protocol.

Single Guide RNA Design

The guide RNA (gRNA) was designed using the *foxq1b* open reading frame sequence. The 20 base pair *foxq1b*-specific gRNA used (5'-GGAGTTGTGCAGCGATGCTG- 3') was followed by an AGG, which is the protospacer adjacent motif (PAM). The gRNA primers were designed to ligate into the pT7-gRNA

plasmid, directly downstream of the T7 promoter. The forward and reverse primers designed to create the gRNA are named zf_foxq1b_gRNA1_L and zf_foxq1b_gRNA1_R. All primers were purchased from Integrated DNA Technologies, and their sequences are found in Table 4.

Annealing of gRNA

The gRNA primers were annealed using 2µl 10X NEB Buffer 3, 2µl zf_foxq1b_gRNA1_L (100µM stock), 2µl zf_foxq1b_gRNA1_R (100µM stock), and 14µl water. The reaction was placed in a thermal cycler set for the following conditions: Primers were heated at 95° C x 5 minutes and the temperature was decreased at a rate of 0.1° C /second down to 50° C; the primers were incubated at 50° C x 10 minutes, after which the temperature was again reduced at a rate of 1° C /second to a final temperature of 4° C.

Ligation of foxq1b gRNA into pT7-gRNA plasmid

The annealed gRNA primers were ligated into the pT7-gRNA plasmid using 1.5µl 10X T4 Buffer, 1µl T4 Ligase (NEB Cat. M0202S), 1µl pT7-gRNA digest, 1µl annealed primers, and 10.5µl water. The reaction was placed in the thermal cycler for 24 hours at 16° C. A transformation was carried out by thawing 50µl of C2925 cells (NEB) on ice for 10 minutes, then adding 1µl of the ligation reaction to the cell tube and flicking gently to mix. The tubes were placed on ice for 30 minutes, and heat shocked for 45 seconds in a 42° C water bath. They were placed back on ice immediately for 5 minutes. 250µl of room temperature S.O.C. media was added to each tube, and the tubes were incubated for 1 hour at 37° C and 250 rpm. 200µl of each tube was spread on pre-warmed agar plates supplemented

with Ampicillin (100µg/ml), and incubated at 37° C for 16 hours. The culturing protocol in the *pT7-gRNA and pT3TS-nCas9n Plasmid DNA Isolation* section was followed. A mini prep was performed following the QIAGEN protocol. The plasmid containing the gRNA specific to *foxq1b* is called *foxq1b*-gRNA.

Restriction digests of foxq1b-gRNA and pT3TS-nCas9n

The *foxq1b*-gRNA plasmid was linearized with *Bam*HI-HF (NEB Cat. R3136S), as previously described. The pT3TS-nCas9n was linearized with *Xba*I (NEB Cat. R0145S). Digests were incubated for 3 hours at 37° C. Afterwards, 1µl 5% SDS, 1µl Proteinase K (100µg/ml) (Sigma Cat. P2308), and 68µl water were added to each digest, and the tubes were incubated for 20 minutes at 55° C to remove any nucleases and contaminating proteins. A phenol-chloroform extraction was performed by adding 100µl of phenol-chloroform (Sigma Cat. P3803) to each of the tubes, and vortexing for 30 seconds. The tubes were centrifuged for 5 minutes at 14K rpm, and the aqueous phase was transferred to a new tube. 10µl (1/10th of product) of 3M Sodium Acetate (pH 5.0) (Fisher Scientific Cat. 127-09-3) was added to each tube and the tubes were vortexed. Afterwards, 300µl (3 volumes of the product) of 100% Ethanol was added to each tube, the tubes were vortexed, and kept on ice for 15 minutes. The tubes were centrifuged at maximum speed (14.8K rpm) for 8 minutes and the supernatant was discarded. The pellets were washed with 500µl of 70% Ethanol and mixed by inversion. The tubes were centrifuged for 5 minutes at 14K rpm and the supernatant was discarded. The pellets were dried and resuspended in 7µl water.

Tyrosinase Control gRNA

As a positive control, the gene tyrosinase (*tyr*) was edited using a tyrosinase gRNA designed by Jao *et al.* (2013). Tyrosinase is essential for the production of melanin and inactivating the locus leads to decreased pigment in chimaeric zebrafish, indicating that the CRISPR technique worked. The double-stranded gRNA, including the gene-specific sequence (5'-GGACTGGAGGACTTCTGGGG-3'), was generated by overlap extension PCR (Bryksin and Matsumura 2010) containing 3µl 10X Hot Master Buffer, 3µl *tyr*_gRNA_L (10µM stock), 3µl *tyr*_gRNA_R (10µM stock), 1µl dNTPs (10mM stock), 0.15µl Hot Master Taq Polymerase (5U/µl) (5 Prime Cat. 2200300), and 19.85µl water. The thermal parameters were: 95^{o} C x 45 seconds; 30 cycles of 95^{o} C x 30 seconds, 55^{o} C x 30 seconds, 72^{o} C x 1 minute; 72^{o} C x 10 minutes. A proteinase K treatment and phenol-chloroform extraction was performed, as previously described.

Transcription of foxq1b-gRNA, tyr-gRNA, and pT3TS-nCas9n

The *foxq1b*-gRNA and *tyr*-gRNA constructs were transcribed using the Life Technologies MEGAshortscriptT7 protocol and kit (Cat. AM1354M), followed by phenol-chloroform extraction and ethanol precipitation. The pT3TS-nCas9n was transcribed using the mMESSAGE mMachine T3 protocol and kit (Cat. AM1348) and precipitated with $LiCl_3$. The final concentration were 2,072ng/µl (*foxq1b* gRNA), 3,638ng/µl ,(*tyr* gRNA) and 673ng/µl (Cas9).

CRISPR Injections

A 5ml 5X stock of the injection mix was made, which contained 600mM KCl (Sigma Cat. P9541), 100mM HEPES pH 7 (Sigma Cat. H3375), and 2.5% v/v phenol red (Sigma Cat. P5530). A final injection mix contained 200ng/µl gRNA (either *foxq1b*-gRNA or *tyr*-gRNA), 150ng/µl Cas9, 1µl 5X injection mix, and water to a final volume of 5µl. 1.5µl of the injection mixture was loaded into a needle, in which the tip was clipped with forceps so that 2-4nl of the final injection mix could be injected into the one cell stage of wild type embryos. AB embryos were used for all injections.

Mutation check through DNA extraction and sequencing

Injected embryos were observed and compared to uninjected embryos at 48 hpf and 72 hpf. Images were taken of the *tyr*-gRNA inject zebrafish at both times points to record the phenotypes. At 72 hpf, images of six embryos injected with the *foxq1b*-gRNA were taken prior to DNA extraction. DNA extraction from whole embryos was performed with 100µl of NTES Mod2, and 1µl of Proteinase K (10mg/ml) at 55^{o} C with continuous rocking until the embryos were completely dissolved (~1 hour). Phenol-chloroform extraction was performed as described. PCR was performed on the extracted DNA using 3µl 10X HotMaster Buffer, 1µl zf_foxq1b_gRNA1check_L (10µM stock), 1µl zF_foxq1b_gRNA1check_R (10µM stock), 1µl dNTPs (10mM stock), 2µl DNA, 0.15µl HotMaster Taq Polymerase (5U/µl), and 21.85µl water. The following thermal parameters were used: 95^{o} C x 45 seconds; 30 cycles of 95^{o} C x 30 seconds, 53^{o} C x 30 seconds, 72^{o} C x 1 minute; 72^{o} C x 10 minutes. Fragments were confirmed on a 2.5% agarose gel and sequenced by the GSL.

Mutation check through qPCR

DNA samples from *foxq1b*-gRNA injected fish described in the previous section, along with DNA from two uninjected zebrafish were quantified using the Qubit dsDNA BR Assay kit (Life Technologies Cat. Q32850). The Agilent Technologies Stratagene Mx3005P was utilized to measure DNA melting curves. Each qPCR tube contained 12.5µl 2X Brilliant II SYBR Green QPCR Master Mix, 0.375µl ROX (1:500), 1µl zf_foxq1b_gRNA1check_L (10µM stock), 1µl zf_foxq1b_gRNA1check_R (10µM stock), 1µl DNA, and 9.125µl water (SYBR Green and ROX were purchased from Stratagene, Cat. 600828). A Comparative Quantitation (Calibrator) qPCR experiment using MxPro software was performed using the following thermal parameters: 95° C x 10 minutes; 40 cycles of 95° C x 30 seconds, 55° C x 30 seconds, 72° C x 30 seconds; 95° C x 1 minute; 55° C x 30 seconds; 95° C x 30 seconds. The melting temperature was determined by measuring fluorescence after each 1° C increase. The melting curves were analyzed and compared to the uninjected controls.

Mutation check through MetaPhor agarose gel

3% MetaPhor agarose (BMA Cat. 50180) was used to analyze amplicons described in *Mutation check through DNA extraction and sequencing*. MetaPhor gels discern fragments that differ by one to two base pairs as a result of gene editing. Eight microliters of the PCR reactions were analyzed. Electrophoresis was carried out at 6V/cm in 4° C 0.5X TBE running buffer (54g Tris Base (Fisher Scientific Cat. 77-86-1), 27.5g Boric acid (Fisher Scientific Cat. 10043-35-3), 20mL 0.5M EDTA (Sigma Cat. 6381-92-6) in 10L water) until the loading dye reached the end of the gel.

Table 4: Primer names and sequence design for gRNA construction.

Primer Name	Sequence (5' - 3')
zf_foxq1b_gRNA1_L	TAGGGGAGTTGTGCAGCGATGCTG
zf_foxq1b_gRNA1_R	AAACCAGCATCGCTGCACAACTCC
tyr_gRNA_L	GAAATTAATACGACTCACTATAGGGGACTGGAGGACTTCTGGGGGTTTTAGAGCTAGAAATAGC
tyr_gRNA_R	AAAAGCACCGACTCGGTGCCACTTTTTCAAGTTGATAACGGACTAGCCTTATTTTAACTTGCTATTTCTAGCTCTAAAAC
zf_foxq1b_gRNA1check_L	TCGAACTTTCTGAAGCTCTGC
zf_foxq1b_gRNA1check_R	TAGGGTTTGCCTTTGGTGTC

Results

CRISPR-Cas technology was used to knockout *foxq1b* in zebrafish. The guide RNA and Cas9 transcripts were injected into the 1-cell stage of wild type zebrafish embryos and the phenotypes were compared to uninjected zebrafish controls. A tyrosinase (*tyr*) gRNA was used as a positive control to assess the efficiency of CRISPR in the injections (Jao 2013). Tyrosinase is a gene in the biosynthetic pathway that converts tyrosine into the pigment melanin. The phenotype of the *tyr*-gRNA injected zebrafish was expected to be lack of pigmentation. The *tyr*-gRNA injections were successful, and phenotypes consisted of a range of pigment production, from faint pigmentation to almost full pigmentation, which was most likely due to chimerism (Figure 10). These results indicated that the Cas9 was working properly.

A *foxq1b*-gRNA, located within the *foxq1b* open reading frame, was designed to knockout *foxq1b* in the zebrafish (Figure 11). It was injected into the 1-cell stage of wild type zebrafish embryos. Since the jaw region of the zebrafish was significantly affected by the *foxq1b* morpholino, this location was initially examined and found to have no distinct differences in jaw structure when compared to uninjected zebrafish at 48 hpf (Figure 12). However, a portion of the population of both the *tyr* and *foxq1b* injected zebrafish resulted in an array of phenotypes. Many of the fish exhibited normal body structure, yet some of the zebrafish exhibited edema, cyclopia, or tail deformities (Figure 13). This made it difficult to distinguish phenotypes that resulted from a *foxq1b* mutation and phenotypes that resulted from the RNA injection process alone.

The DNA was extracted from six of the *foxq1b*-gRNA injected fish and a PCR was performed with primers that spanned the gRNA region. The PCR reactions were sent for sequencing, and none of the sequences contained a mutation in this region. The fact that no distinct sequence alterations were apparent could be due to chimerism, where *foxq1b* was only successfully altered by CRISPR in a portion of the cells. This would result in a phenotype with no significant abnormalities, and allow the endogenous sequence to be most frequently observed by sequencing.

Since the sequences didn't show any significant changes in the gene, qPCR was performed using the DNA that was extracted from the six *foxq1b*-gRNA injected zebrafish to observe any differences in the melting curves. The melting curve assesses the dissociation of the double stranded DNA as the temperature is increased. This allows for any single-nucleotide polymorphisms (SNPs) and insertions or deletions to be detected. Two out of the six *foxq1b*-gRNA injected zebrafish exhibited melting curves that deviated from the uninjected zebrafish melting curves (Figure 14). This indicates the possibility that some of the cells were mutagenized by the *foxq1b*-gRNA.

The PCR reactions containing DNA from the six *foxq1b*-gRNA injected zebrafish and the primer pair that flanked the *foxq1b*-gRNA region were run on a 3% MetaPhor agarose gel to discern base pair differences that might have arisen due to a CRISPR mutations within the *foxq1b* gene. Amplicons from five of the six *foxq1b*-gRNA injected zebrafish produced multiple fragments of different sizes when compared to uninjected zebrafish (Figure 15). These results indicate the likelihood that other fish in the same cohort contain mutations

within the *foxq1b* gene; therefore, the remainder will be raised to adulthood and crossed with wild-type to select for the *foxq1b*-gRNA injected fish that contain mutations within the germ line. The fish in the F1 generation that are heterozygous for the *foxq1b* mutation will be intercrossed in order to obtain a null *foxq1b* zebrafish line.

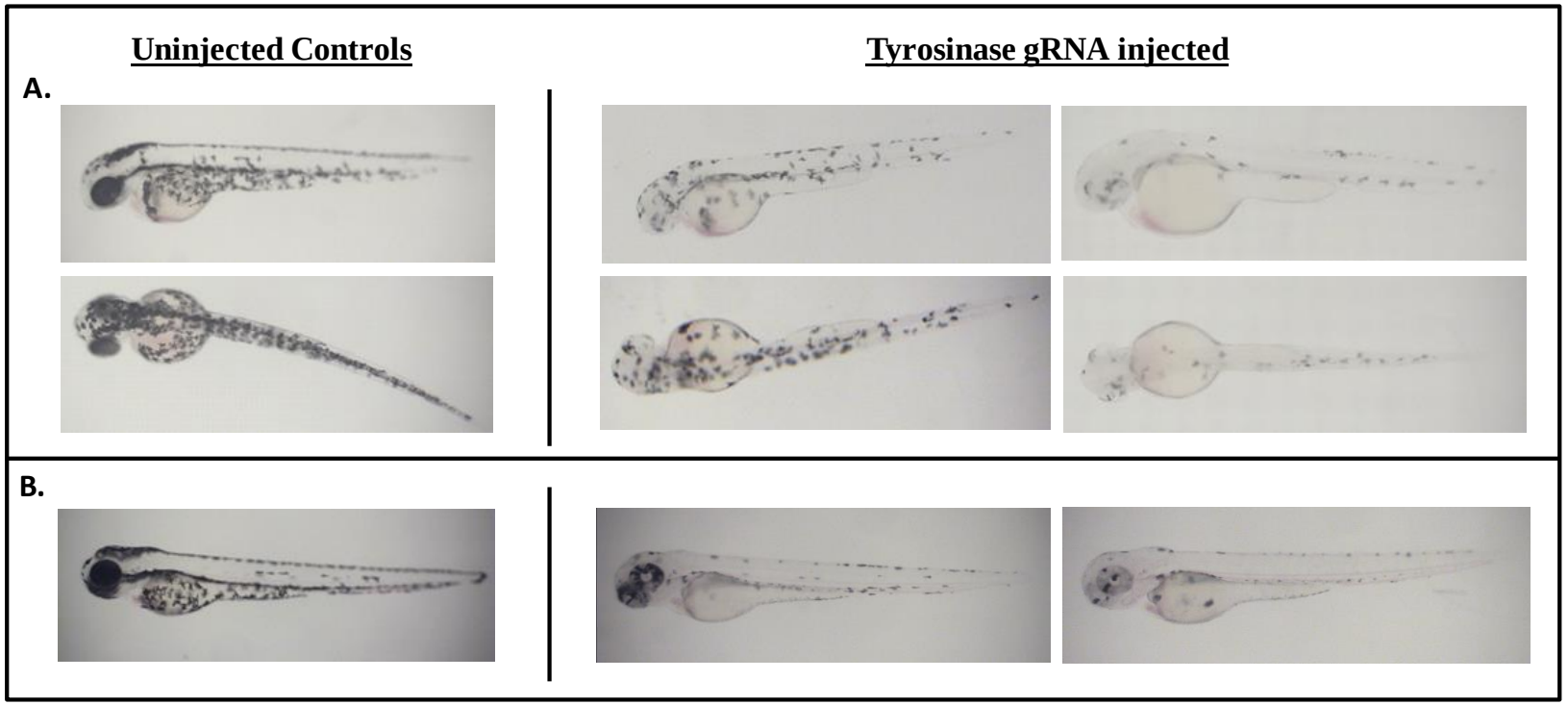

Figure 10: Tyrosinase-gRNA injected vs. uninjected zebrafish. A. 48 hpf uninjected control zebrafish compared to 48 hpf *tyr*-gRNA injected zebrafish. Both lateral and dorsal views are shown. **B.** 72 hpf uninjected control zebrafish compared to 72 hpf *tyr*-gRNA injected zebrafish. *Since there are varying degrees of pigment formation within the zebrafish injected with *tyr*-RNA, multiple phenotypes are shown.

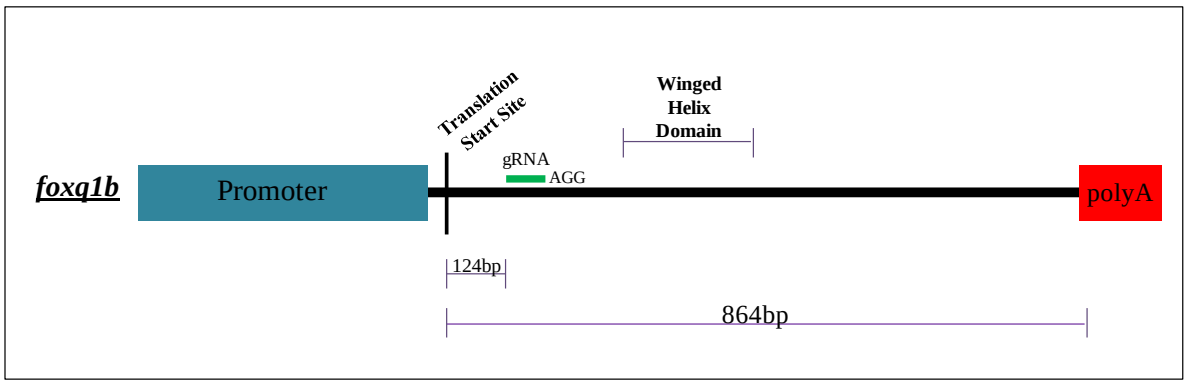

Figure 11: *Foxq1b*-gRNA design. The location of the 20 base pair *foxq1b*-gRNA within the *foxq1b* gene in relation to the start site of translation.

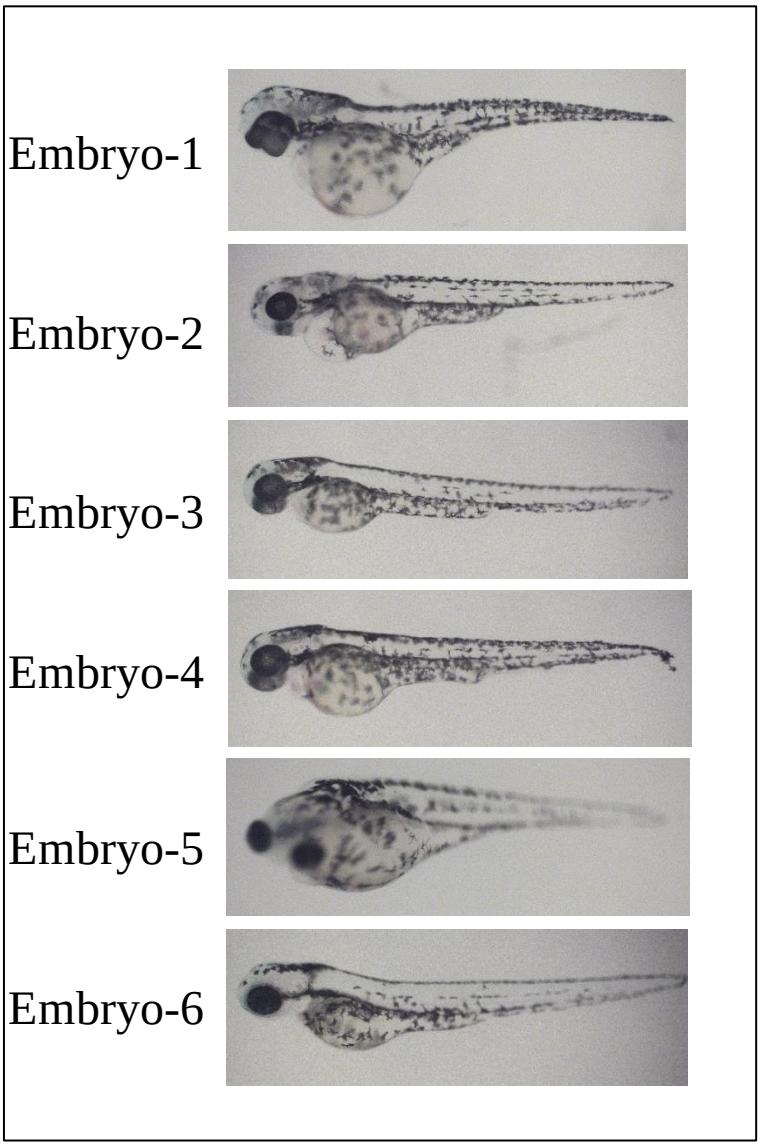

Figure 12: *Foxq1b*-gRNA injected zebrafish. The zebrafish labeled 1-6 are the *foxq1b*-gRNA injected fish that were imaged and DNA extracted at 72 hpf to determine if any potential mutations in *foxq1b* occurred.

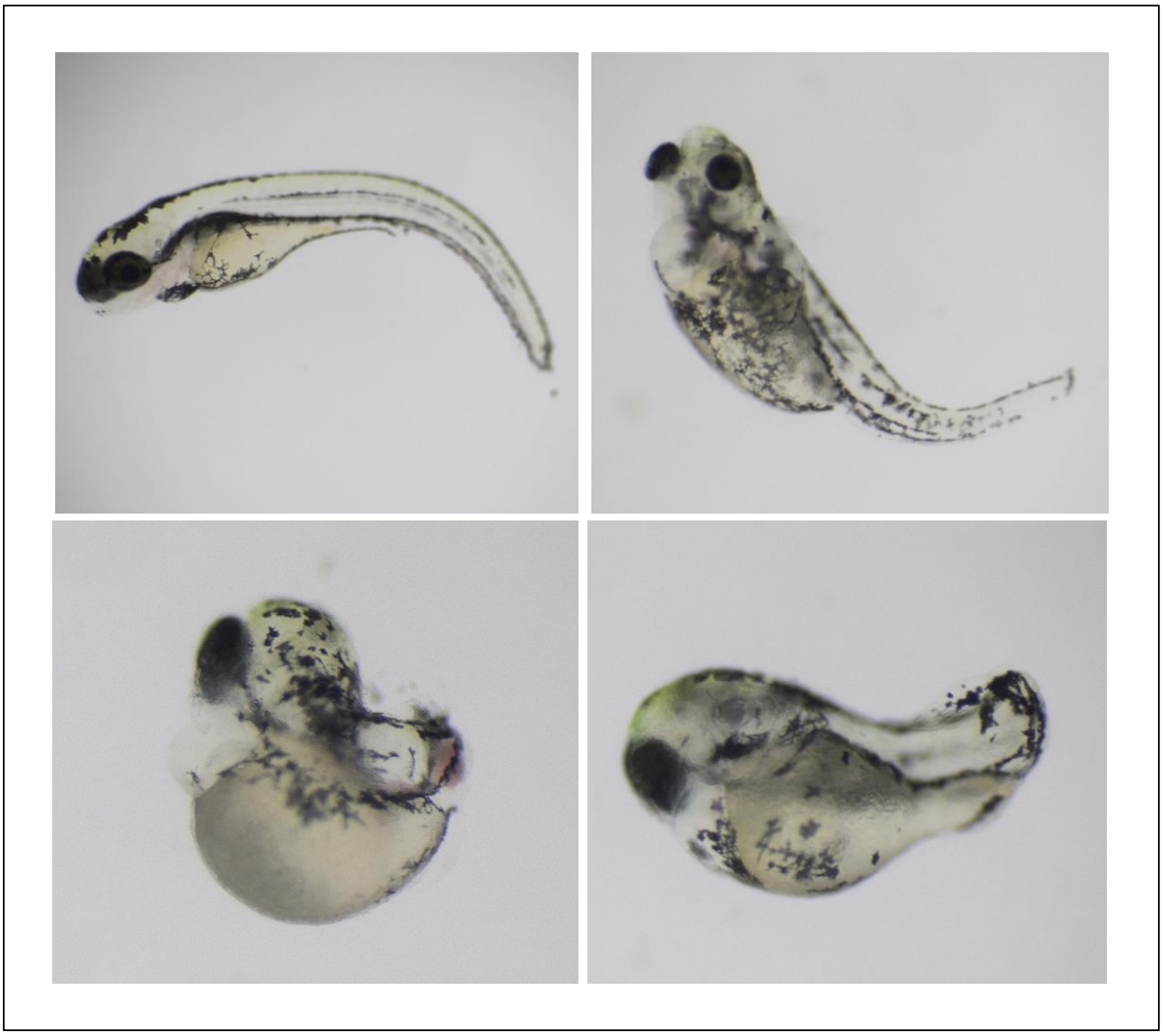

Figure 13: Abnormal *foxq1b*-gRNA injected zebrafish. 48 hpf zebrafish that were injected with *foxq1b*-gRNA at the 1-cell stage. The injection of RNA seems to cause a range of abnormalities that are unrelated to the mutations that would be derived from the gRNA.

Figure 14: qPCR melting curves of *foxq1b*-gRNA injected compared to uninjected zebrafish. A. The -Rn'(T) and R (Multicomponent view) melting curves for all six *foxq1b*-gRNA injected zebrafish compared to the melting curve of two uninjected control zebrafish (WT). **B.** The two melting curves that deviated from the uninjected melting curves. The -Rn'(T), which is the negative of the first derivative based on the normalized fluorescence, and R (Multicomponent view) melting curves for *foxq1b*-gRNA injected embyro-1 and *foxq1b*-gRNA injected embryo-4 compared to the two uninjected controls.

A.

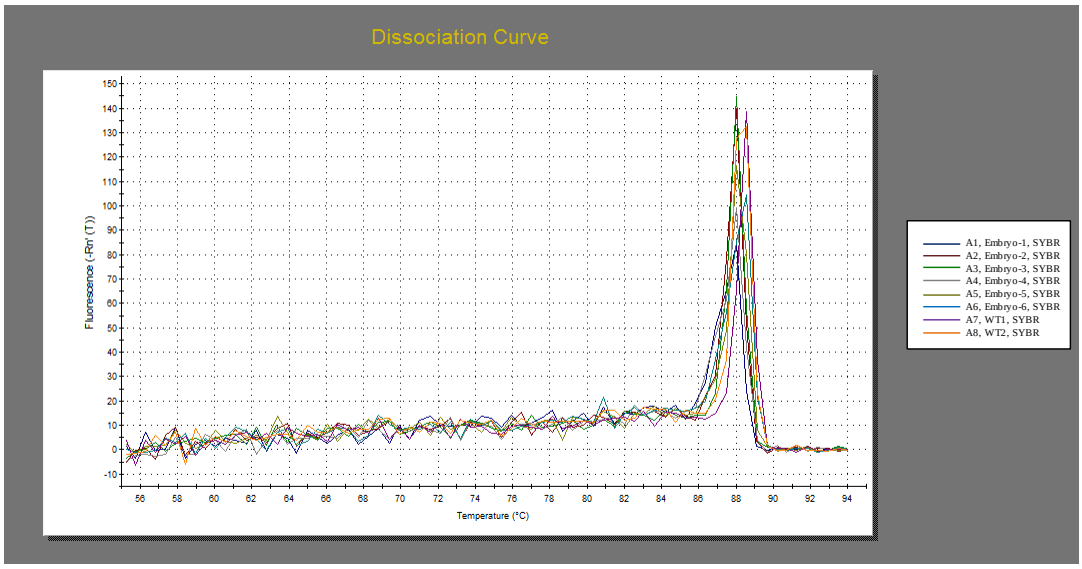
Dissociation Curve
Fluorescence (-Rn' (T))
Temperature (°C)
A1, Embryo-1, SYBR
A2, Embryo-2, SYBR
A3, Embryo-3, SYBR
A4, Embryo-4, SYBR
A5, Embryo-5, SYBR
A6, Embryo-6, SYBR
A7, WT1, SYBR
A8, WT2, SYBR

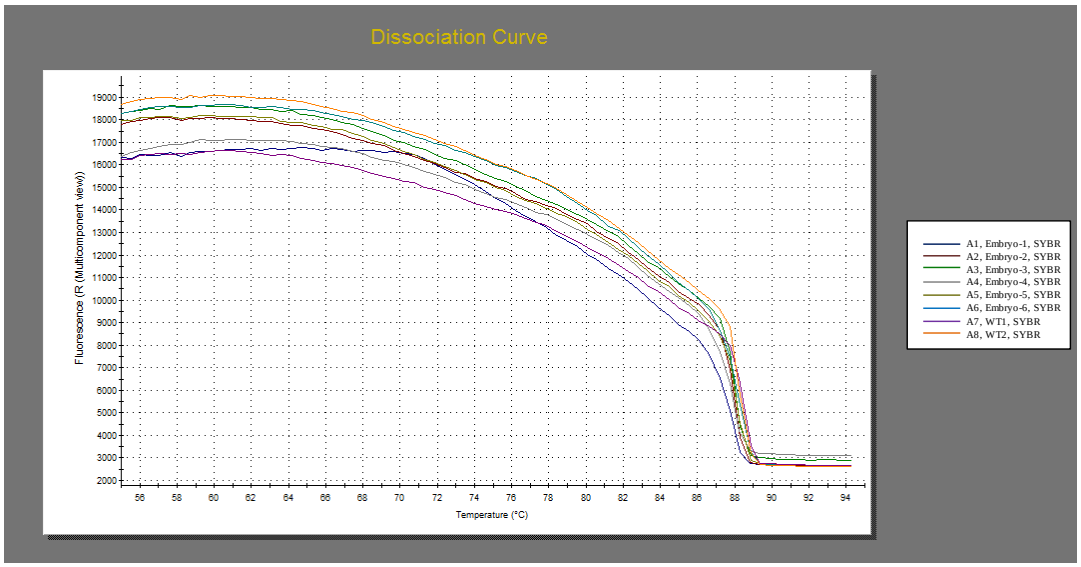
Dissociation Curve
Fluorescence (R (Multicomponent view))
Temperature (°C)
A1, Embryo-1, SYBR
A2, Embryo-2, SYBR
A3, Embryo-3, SYBR
A4, Embryo-4, SYBR
A5, Embryo-5, SYBR
A6, Embryo-6, SYBR
A7, WT1, SYBR
A8, WT2, SYBR

B.

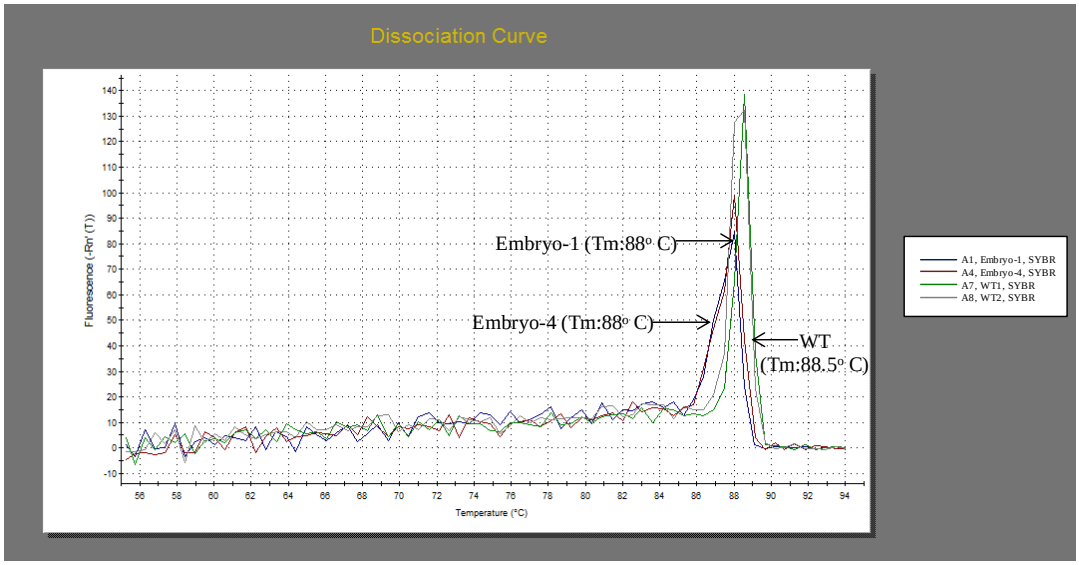
Dissociation Curve
Fluorescence (-Rn' (T))
Temperature (°C)
Embryo-1 (Tm:88° C)
Embryo-4 (Tm:88° C)
WT
(Tm:88.5° C)
A1, Embryo-1, SYBR
A4, Embryo-4, SYBR
A7, WT1, SYBR
A8, WT2, SYBR

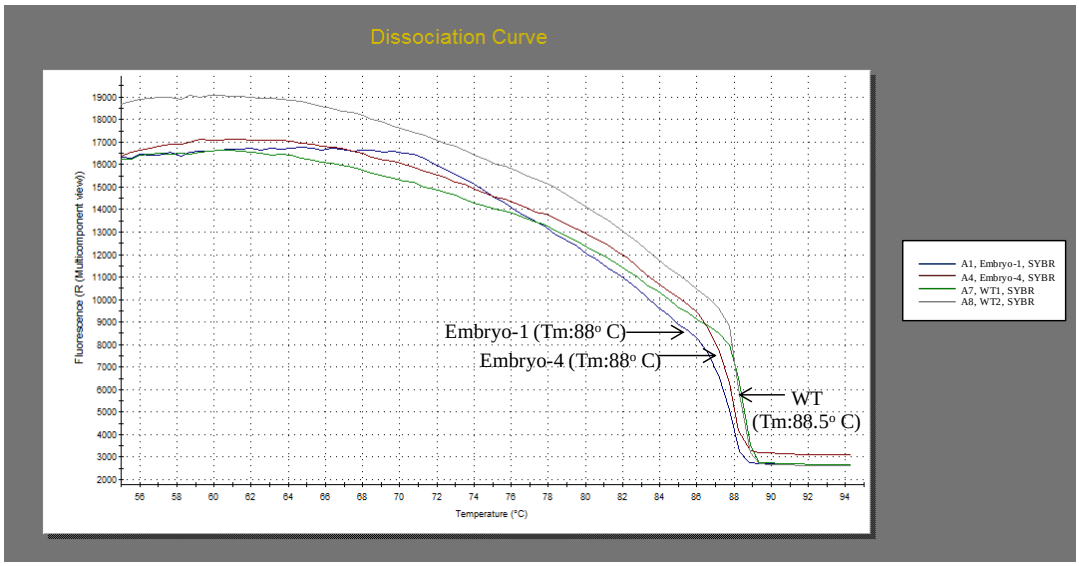
Dissociation Curve
Fluorescence (R (Multicomponent view))
Temperature (°C)
Embryo-1 (Tm:88° C)
Embryo-4 (Tm:88° C)
WT
(Tm:88.5° C)
A1, Embryo-1, SYBR
A4, Embryo-4, SYBR
A7, WT1, SYBR
A8, WT2, SYBR

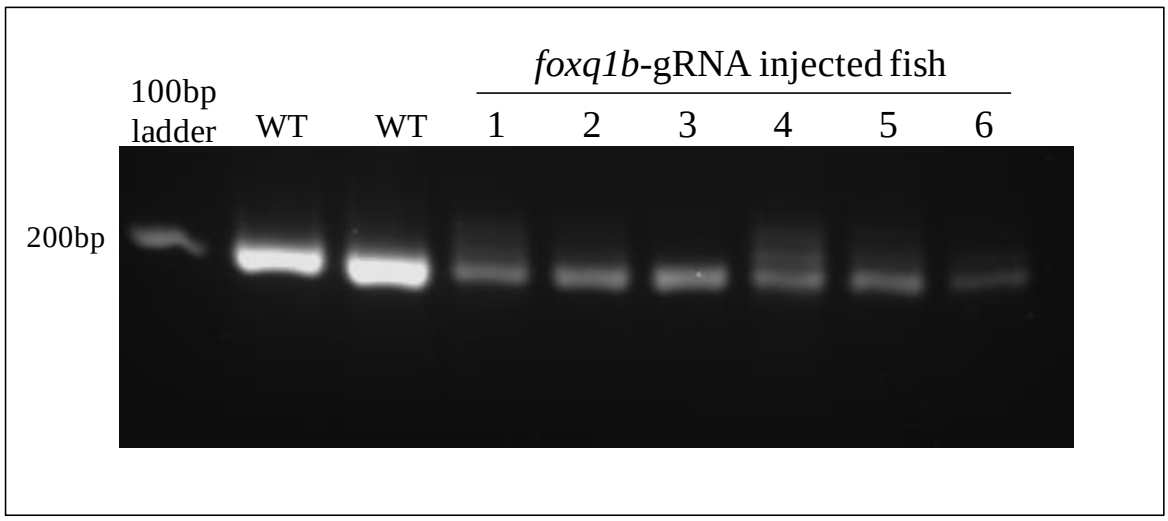

Figure 15: MetaPhor gel of *foxq1b*-gRNA injected zebrafish compared to uninjected controls. The DNA from six fish, whose melting curves were examined via qPCR, was analyzed on a 3% MetaPhor agarose gel to determine if the *foxq1b*-gRNA altered any sequences compared to the uninjected wild type zebrafish. *Foxq1b*-gRNA injected zebrafish 1,2,4,5, and 6 appear to contain multiple fragments compared to the WT controls.

Discussion

FOXQ1 has been shown to be important in many aspects of mammalian embryonic development, including craniofacial formation (Goering 2008). A knockdown of *foxq1b* in zebrafish through the use of a morpholino, which resulted in abnormal jaw structure, has further shown *foxq1b's* significance throughout development. However, it is unclear whether *foxq1b* is required for survival. Using CRISPR-Cas technology, a *foxq1b* knockout can be generated in order to observe resulting phenotypic effects.

The CRISPR injections appeared to be successful since the *tyr*-gRNA injection significantly decreased pigment production within the zebrafish. Tyrosinase is a good control gene for CRISPR because mutations within this gene produce easily observed phenotypes. Although the *tyr*-gRNA and Cas9 significantly reduced pigmentation in the injected zebrafish, total pigment was not lost. Instead, the phenotype consisted of a mosaic pattern, meaning that tyrosinase was not completely knocked out of every cell. Similar mosaic results were observed when the Yen lab injected *tyr*-gRNA into the one cell stage of zebrafish and *Xenopus* embryos. However, when *tyr*-gRNA was injected into mouse embryos, at least one mouse was completely albino (Yen 2014). Since zebrafish are a rapidly developing organism, the translation of Cas9 might occur after cell division has already taking place, where as in mice, the two cell stage occurs 24 hours after fertilization, giving Cas9 significantly more time to undergo translation (Yen 2014). When observing the *foxq1b*-gRNA and Cas9 injected embryos, distinct phenotypes were difficult to detect due to the presence of abnormal phenotypes from RNA injection alone. Since no conclusive phenotype

was found in the *foxq1b*-gRNA injected zebrafish and a mosaic phenotype was present within the *tyr*-gRNA injected zebrafish, chimerism may have taken place, where only a portion of the cells are mutated by CRISPR due to the delayed translation of Cas9.

Although no phenotypic abnormalities (apart from RNA injection alone) were observed in embryos derived from the *foxq1b*-gRNA and Cas9 injections, genotypic analysis showed the presence of potential *foxq1b* mutations. The melting curves of the DNA from six *foxq1b*-gRNA injected embryos were examined, and the DNA fragments from two of the six appeared to dissociate at a lower temperature than the uninjected wild type zebrafish. Further investigation using a MetaPhor agarose gel, which can resolve DNA fragments differing by as little as 2 base pairs in a 100 base pair amplicon, showed the presence of multiple fragments in the *foxq1b*-gRNA injected DNA when compared to the uninjected wild type DNA. These mutations may take place in only a small fraction of the cells since they were not detected through sequencing, but if they are present in the germ line the mutations are likely to be passed to future generations.

The *foxq1b*-gRNA injected fish will be reared to adulthood. The F_0 population will be crossed with wild type zebrafish to determine if the *foxq1b* mutations are heritable. Subsequent steps include intercrosses of heterozygous carriers to produce a homozygous *foxq1b* knockout. The *foxq1b* mutant line will determine the severity of a *foxq1b* null on proper embryonic development. This research will be valuable towards the study of craniofacial abnormalities, and the role *FOXQ1* plays in the development of facial features.

These knockout zebrafish can also be utilized to determine what important genes and pathways are disrupted due to the lack of *foxq1b* expression in both development and cancer.

Conclusion

Craniofacial abnormalities are a common type of birth defect. Much is still unknown about the genetic mutations that can lead to facial defects. *FOXQ1* is known to play an important role in cranial development in both mammals and zebrafish. Utilizing a *foxq1b* knockout through CRISPR-Cas9 technology will determine to what degree *foxq1b* is required for proper craniofacial development, and how altered expression of *foxq1b* affects other pathways involved in development. This research could provide greater knowledge and potential treatments for craniofacial abnormalities in humans. It can also be used to observe genes involved in cancer that are affected due to a *foxq1b* knockout, which could be beneficial for the cancer research community.

REFERENCES

Abba, M., Patil, N., Rasheed, K., Nelson, L. D., Mudduluru, G., Leupold, J. H., and H. Allgayer. 2013. Unraveling the role of FOXQ1 in colorectal cancer metastasis. American Association for Cancer Research. 1-33.

Agarwal, M. L., Agarwal, A., Taylor, W. R., and G. R. Stark. 1995. p53 controls both the G_2/M and the G_1 cell cycle checkpoints and mediates reversible growth arrest in human fibroblasts. Cell Biology. 92:8493-8497.

Bao, B., Azmi, A.S., Aboukameel, A., Ahmad, A., Bolling-Fischer, A., Sethi, S., Ali, S., Li, Y., Kong, D., Banerjee, S., Back, J., and F. H. Sarlar. Pancreatic cancer stem-like cells display aggressive behavior mediated via activation of FoxQ1. 2014. J Biol Chem. 21:14520-14533.

Bennett, W. P., Hussain, S. P., Vahakangas, K. H., Khan, M. A., Shields, P. G., and C. C. Harris. 1999. Molecular Epidemiology of Human Cancer Risk: Gene-Environment Interactions and *p53* Mutation Spectrum in Human Lung Cancer. J. Pathol. 187:8-18.

Bieller, A., Pasche, B., Frank, S., Glaser, B., Kunz, J., Witt, K., and B. Zoll. 2001. Isolation and Characterization of the Human Forkhead Gene FOXQ1. DNA and Cell Biology. 20:555-561.

Brill, A., Torchinsky, A., Carp, H., and V. Toder. 1999. The Role of Apoptosis in Normal and Abnormal Embryonic Development. Journal of Assisted Reproduction and Genetics. 16:512-519.

Brosh, R., Sarig, R., Natan, E. B., Molchadsky, A., Madar, S., Bornstein, C., Buganim, Y., Shapira, T., Goldfinger, N., Paus, R., and V. Rotter. 2010. p53-dependent transcriptional regulation of EDA2R and its involvement in chemotherapy-induced hair loss. FEBS Letters. 584:2473-2477.

Bryksin, A. V., and I. Matsumura. 2010. Overlap extension PCR cloning: a simple and reliable way to create recombinant plasmids. Biotechniques. 48:463-465.

Carlsson, P., and M. Mahlapuu. 2002. Forkhead transcription factors: key players in development and metabolism. Dev. Biol. 250:1-23.

Carney, T. J., Dutton, K. A., Greenhill, E., Delfino-Machin, M., Dufourcq, P., Blader, P., and R. N. Kelsh. 2006. A direct role for Sox10 in specification of neural crest-derived sensory neurons. Development. 133:4619-4630.

Cerny, R., Cattell, M., Sauka-Spengler, T., Bronner-Fraser, M., Yu, F., and D. M. Medeiros. 2010. Evidence for the prepattern/cooption model of vertebrate jaw evolution. Proc Natl Acad Sci USA. 107:17262-17267.

Chen, J., Ng, S. M., Chang, C., Zhang, Z., Bourdon, J., Lane, D. P., and J. Peng. 2009. p53 isoform Δ113p53 is a p53 target gene that antagonizes p53 apoptotic activity via BclxL activation in zebrafish. Genes & Development. 23:278-290.

Chen, M., and J. Wang. 2002. Initiator caspases in apoptosis signaling pathways. Apoptosis. 7:313-319.

Choi, V.M., Harland, R. M., and M. K. Khokha. 2006. Developmental expression of FoxJ1.2, FoxJ2, and FoxQ1 in *Xenopus tropicalis*. Gene Expression Patterns. 6:443-447.

Christensen, J., Bentz, S., Sengstag, T., Shastri, V. P., and P. Anderle. 2013. FOXQ1, a Novel Target of the Wnt Pathway and a New Marker for Activation of Wnt Signaling in Solid Tumors. PLOS ONE. 8:1-10.

Crow, K. D., Wagner, G. P. 2006. What Is the Role of Genome Duplication in the Evolution of Complexity and Diversity? Mol. Biol. Evol. 23:887-892.

Daniels, D. L., and W. I. Weis. 2005. Beta-catenin directly displaces Groucho/TLE repressors from Tcf/Lef in Wnt-mediated transcription activation. Nat Struct Mol Biol. 4:364-371.

Deltcheva, E., Chylinski, K., Sharma, C. M., Gonzales, K., Chao, Y., Pirzada, Z. A., Eckert, M. R., Vogel, J., and E. Charpentier. 2011. CRISPR RNA maturation by trans-encoded small RNA and host factor RNase III. Nature. 471:602-607.

Dere, E., Lee, A. W., Burgoon, L. D., and T. R. Zacharewski. 2011. Differences in TCDD-elicited gene expression profiles in human HepG2, mouse Hepalclc7 and rat H4IIE hepatoma cells. BMC Genomics. 12:193.

Driskell, R. R., Clavel, C., Rendl, M., and F. M. Watt. 2011. Hair follicle dermal papilla cells at a glance. Journal of Cell Science. 124:1179-1182.

Faust, D., Vondracek, J., Krcmar, P., Smerdova, L., Prochazkova, J., Hruba, E., Hulkinkova, P., Kaina, B., Dietrich, C., and M. Machala. 2013. AhR-mediated changes in global gene expression in rat liver progenitor cells. Arch. Toxicol. 87:681-698.

Feng, J., Xu, L., Ni, S., Gu, J., Zhu, H., Wang, H., Zhang, S., Zhang, W., and J. Huang. 2014. Involvement of FoxQ1 in NSCLC through regulating EMT and increasing chemosensitivity. Oncotarget. 5:9689-9702.

Feuerborn, A., Srivastava, P. K., Kuffer, S., Grandy, W. A., Sijmonsma, T. P., Gretz, N., Brors, B., and H. -J. Grone. 2011. The Forkhead Factor FoxQ1 Influences Epithelial Differentiation. J. Cell. Physiol. 226:710-719.

Francis-West, P. H., Robson, L, and D. J. Evans. 2003. Craniofacial development: the tissue and molecular interactions that control development of the head. Adv Anat Embryol Cell Biol. 169:1-138.

Gao, M., Shih, I., and T. Wang. 2012. The Role of Forkhead Box Q1 Transcription Factor in Ovarian Epithelial Carcinomas. In. J. Mol. Sci. 13:13881-13893.

Godwin, A. R., and M. R. Capecchi. 1998. Hoxc13 mutant mice lack external hair. Genes Dev. 12:11-20.

Goering, W., Adham, I. M., Pasche, B., Manner, J., Ochs, M., Engel, W., and B. Zoll. 2008. Impairment of gastric acid secretion and increase of embryonic lethality in *Foxq1*-deficient mice. Cytogenet Genome Res. 121:88-95.

Graham, A., Okabe, M., and R. Quinlan. 2005. The role of the endoderm in the development and evolution of the pharyngeal arches. J. Anat. 207:479-487.

Gumbiner, B. M. 1996. Cell adhesion: the molecular basis of tissue architecture and morphogenesis. Cell. 84:345-357.

Hannenhalli, S., and K. H. Kaestner. 2009. The evolution of Fox genes and their role in development and disease. Nat Rev Genet. 10:233-240.

Hoggatt, A. M., Kriegel, A. M., Smith, A. F., and B. P. Herring. 2000. Hepatocyte Nuclear Factor-3 Homologue 1 (HFH-1) Represses Transcription of Smooth Muscle-specific Genes. The Journal of Biological Chemistry. 275:31162-31170.

Hong, H., Noveroske, J. K., Headon, D. J., Liu, T., Sy, M., Justice, M. J., and A. Chakravarti. 2001. The Winged Helix/Forkhead Transcription Factor *Foxq1* Regulates Differentiation of Hair in Satin Mice. Genesis. 29:163-171.

Jackson, M. W., Agarwal, M. K., Yang, J., Bruss, P., Uchiumi, T., Agarwal, M. L, Stark, G. R., and W. R. Taylor. 2005. p130/p107/p105Rb-dependent transcriptional repression during DNA-damage-induced cell-cycle exit at G2. J Cell Sci. 118:1821-1832.

Jao, L., Wente, S. R., and W. Chen. 2013. Efficient multiplex biallelic zebrafish genome editing using a CRISPR nuclease system. PNAS. 110:13904-13909.

Jechlinger, M., Sommer, A., Moriggl, R., Seither, P., Kraut, N., Capodiecci, P., Donovan, M., Cordon-Cardo, C., Beug, H., and S. Grunert. 2006. Autocrine

PDGRF signaling promotes mammary cancer metastasis. J. Clin. Invest. 116:1561-1570.

Jiang, W., Bikard, D., Cox, D., Zhang, F., and L. A. Marraffini. 2013. RNA-guided editing of bacterial genomes using CRISPR-Cas systems. Nat Biotechnol. 31:233-239.

Jin, Y. R., Turcotte, T. J., Crocker, A. L., Han, X. H., and J. K. Yoon. 2011. The canonical Wnt signaling activator, R-spondin2, regulates craniofacial patterning and morphogenesis within the branchial arch through ectodermal-mesenchymal interaction. Dev Biol. 352:1-13.

Jinek, M., Chylinski, K., Fonfara, I., Hauer, M., Doudna, J. A., and E. Charpentier. 2012. A programmable dual-RNA-guided DNA endonuclease in adaptive bacterial immunity. Science. 337:816-821.

Jonsson, H., and S.L. Peng. 2005. Forkhead transcription factors in immunology. Cell. Mol. Life Sci. 62:397-409.

Kaneda, H., Arao, T., Tamua, D., Aomatsu, K., Kudo, K., Sakai, K., Velasco, M., Matsumoto, K., Fujita, Y., Yamada, Y., Tsurutani, J., Okamoto, I., Nakagawa, K., and K. Nishio. 2010. FOXQ1 Is Overexpressed in Colorectal Cancer and Enhances Tumorigenicity and Tumor Growth. Cancer Res. 70:2053-2063.

Katoh, Y., and M. Katoh. 2008. Integrative genomic analyses on GLI2: Mechanism of Hedgehog priming through basal GLI2 expression, and interaction map of stem cell signaling network with P53. International Journal of Oncology. 33:881-886.

Kere, J., Srivastava, A. K., Montonen, O., Zonana, J., Thomas, N., Ferguson, B., Munoz, F., Morgan, D., Clarke, A., Baybayan, P., Chen, E. Y., Ezer, S., Saarialho-Kere, U., de la Chapelle, A., and D. Schlessinger. 1996. X-linked anhidrotic (hypohidrotic) ectodermal dysplasia is caused by mutation in a novel transmembrane protein. Nat Genet. 13:409–416.

Kuroiwa, Y., Nishikawa, A., Kitamura, Y., Kanki, K., Ishii, Y., Umemura, T., and M. Hirose. 2006. Protective effects of benzyl isothiocyanate and sulforaphane but not resveratrol against initiation of pancreatic carcinogenesis in hamsters. Cancer Lett. 241:275-280.

Le, P. N., McDermott, J. D., and A. Jimeno. 2014. Targeting the Wnt pathway in human cancers: Therapeutic targeting with a focus on OMP-54F28. Pharmacol. Ther. 14:162-164.

Li, L., and W. Li. 2015. Epithelial-mesenchymal transition in human cancer: Comprehensive reprogramming of metabolism, epigenetics, and differentiation. Pharmacology and Therapeutics. 1-69.

Logan, C. Y., and R. Nusse. 2004. The Wnt Signaling Pathway in Development and Disease. Annu. Rev. Cell Dev. Biol. 20:781-810.

Lusska, A., Shen, E., and J. P. Whitlock Jr. 1993. Protein-DNA interactions at a dioxin-responsive enhancer. J. Biol. Chem. 268:6575-6580.

Lynch, M., and J. S. Conery. 2000. The evolutionary fate and consequences of duplicate genes. Science. 290:1151-1155.

Martinez-Ceballos, E., Chambon, P., and L. J. Gudas. 2005. Differences in Gene Expression between Wild Type and Hoxa1 Knockout Embryonic Stem Cells after Retinoic Acid Treatment or Leukemia Inhibitory Factor (LIF) Removal. The Journal of Biological Chemistry. 280:16484-16498.

Mazet, F., Luke, G. N., and S. M. Shimeld. 2005. The amphioxus *FoxQ1* gene is expressed in the developing endostyle. Gene Expr. Patterns. 5:313-315.

McConnell, K. W., and C. M. Coopersmith. 2005. Epithelial Cells. Crit Care Med. 33:S520-S522.

Meng, F., Speyer, C., Zhang, B., Zhao, Y., Chen, W., Gorski, D., Miller, F. R., and G. Wu. 2014. PDGFRα and β Play Critical Roles in Mediating Foxq1-Driven Breast Cancer Stemness and Chemoresistance. Cancer Res. 1-22.

Momand, J., Zambetti, G. P., Olson, D. C., George, D., and A. J. Levine. 1992. The mdm-2 oncogene product forms a complex with the p53 protein and inhibits p53-mediated transactivation. Cell. 69:1237-1245.

Nieuwkoop, P. D., and J. Faber. 1994. Normal Table of *Xenopus laevis* (Daudin). Garland Publishing Inc, New York. ISBN 0-8153-1896-0.

Ogasawara, M., and Y. Satou. 2003. Expression of FoxE and FoxQ genes in the endostyle of Ciona intestinalis. Dev. Genes Evol. 213:416-419.

Pearson, J. C., Lemons, D., and W. McGinnis. 2005. Modulating Hox Gene Functions during Animal Body Patterning. Nature Reviews. 6:893-904.

Peng, X. H., Huang, H. R., Lu, X., Zhao, F. P., Zhang, B., Lin, S. X., Wang, L., Chen, H. H., Xu, X., Wang, F., and X. P. Li. 2014. MiR-124 suppresses tumor growth and metastasis by targeting Foxq1 in nasopharyngeal carcinoma. Molecular Cancer. 13:1-13.

Piavis, G. W. 1960. Embryological Stages in the Sea Lamprey and Effects of Temperature on Development. Fishery Bulletin. 182:111-143.

Planchart, A., and C. Mattingly. 2010. 2,3,7,8-Tetrachlorodibenzo-*p*-dioxin Upregulates FoxQ1b in Zebrafish Jaw Primordium. Chem. Res. Toxicol. 23:450-487.

Postlethwait, J., Yan, Y., Gates, M., Horne, S., Amores, A., Brownlie, A., Donovan, A., Egan, E., Force, A., Gong, Z., Goutel, C., Fritz, A., Kelsh, R., Knapik, E., Liao, E., Paw, B., Ransom, D., Singer, A., Thomson, M., Abduljabbar, T. S., Yelick, P., Beier, D., Joly, J.-S., Larhammar, D., Rosa, F., Westerfield, M., Zon, L. I., Johnson, S. L., and W. S. Talbot. 1998. Vertebrate genome evolution and the zebrafish gene map. Nature genetics. 18:345-349.

Potter, C. S., Peterson, R. L., Barth, J. L., Pruett, N. D., Jacobs, D. F., Kern, M. J., Argraves, W. S., Sundberg, J. P., and A. Awgulewitsch. 2006. Evidence That the Satin Hair Mutant Gene *Foxq1* Is among Multiple and Functionally Divers Regulatory Targets for *Hoxc13* during Hair Follicle Differentiation. J. Biol. Chem. 281:29245-29255.

Presgraves, D. C. 2005. Evolutionary genomics: New genes for new jobs. Current Biology. 15:R52-R53.

Qiao, Y., Jiang, X. Lee, S. T., Karuturi, R. K., Hooi, S. C., and Q. Yu. 2011. FOXQ1 Regulates Epithelial-Mesenchymal Transition in Human Cancers. Cancer Res. 71:3076-3086.

Rashid, N. N., Yusof, R., and R. J. Watson. 2011. Disruption of repressive p130-DREAM complexes by human papillomavirus 16 E6/E7 oncoproteins is required for cell-cycle progression in cervical cancer cells. Journal of General Virology. 92:2620-2627.

Sehrawat, A., and S. V. Singh. 2011. Benzyl isothiocyanate inhibits epithelial-mesenchymal transition in cultured and xenografted human breast cancer cells. Cancer Prev. Res. 4:1107-1117.

Sehrawat, A., Kim, S., Vogt, A., and S. V. Singh. 2013. Suppression of FOXQ1 in benzyl isothiocyanate-mediated inhibition of epithelial-mesenchymal transition in human breast cancer cells. Carcinogenesis. 34:864-873.

Siegel, R., Ma, J., Zou, Z., and A. Jemal. 2014. Cancer Statistics, 2014. A Cancer Journal for Clinicians. 64:9-29.

Sternberg, S. H., Redding, S., Jinek, M., Greene, E. C., and J. A. Doudna. 2014. DNA interrogation by the CRISPR RNA-guided endonuclease Cas9. Nature. 507:62-67.

Stevens, E. A., Mezrich, D., and C. A. Bradfield. 2009. The aryl hydrocarbon receptor: a perspective on potential roles in the immune system. Immunology. 127:299-311.

Sun, H., Cheng, S., Tu, Y., Li, X., and S. Zhang. 2013. FoxQ1 Promotes Glioma Cells Proliferation and Migration by Regulating NRXN3 Expression. PLOS ONE. 8:1-8.

Tanikawa, C., Ri, C., Kumar, V., Nakamura, Y., and K. Matsuda. 2010. Crosstalk of EDA-A2/XEDAR in the p53 Signaling Pathway. Molecular Cancer Research. 8:855-863.

Thornley, J. A., Trask, H. W., Ridley, C. J. A., Korc, M., Gui, J., Ringelberg, C. S., Wang, S., and C. R. Tomlison. 2011. Differential regulation of polysome mRNA levels in mouse Hepa-1C1C7 cells exposed to dioxin. Toxicology in Vitro. 25:1457-1467.

Tkatchenko, A. V., Visconti, R. P., Shang, L., Papenbrock, T., Pruett, N. D., Ito, T., Ogawa, M., and A. Awgulewitsch. 2001. Overexpression of Hoxc13 in differentiating keratinocytes results in downregulation of a novel hair keratin gene cluster and alopecia. Development. 128:1547-1558.

Vanderas, A.P. 1987. Incidence of cleft lip, cleft palate, and cleft lip and palate among races: a review. Cleft Palate J. 24:216-225.

Verzi, M. P., Khan, A. H., Ito, S., and R. A. Shivdasani. 2008. Transcription Factor Foxq1 Controls Mucin Gene Expression and Granule Content in Mouse Stomach Surface Mucous Cells. Gastroenterology. 135:591-600.

Warin, R., Chambers, W. H., Potter, D. M., and S. V. Singh. 2009. Prevention of mammary carcinogenesis in MMTV-neu mice by cruciferous vegetable constituent benzyl isothiocyanate. Cancer Res. 69:9473-9480.

Wazir, U., Orakzai, M. M., Khanzada, Z. S., Jiang, W. G., Sharma, A. K., Kasem, A., and K. Mokbel. 2015. The role of death-associated protein 3 in apoptosis, anoikis and human cancer. Cancer Cell International. 15:1-10.

Weigel, D., Jürgens, G., Küttner, F., Seifert, E., and H. Jackle. 1989. The homeotic gene *fork head* encodes a nuclear protein and is expressed in the terminal regions of the Drosophila embryo.

Wotton, K., and S. Shimeld. 2011. Analysis of lamprey clustered Fox genes: Insight into Fox gene evolution and expression in vertebrates. Gene. 489:30-40.

Xia, L., Huang, W., Tian, D., Zhang, L., Qi, X., Chen, Z., Shang, X., Nie, Y., and K. Wu. 2014. Forkhead Box Q1 Promotes Hepatocellular Carcinoma Metastasis by Transactivating ZEB2 and VersicanV1 Expression. Hepatology. 59:958-973.

Yaklichkin, S., Vekker, A., Stayrook, S., Lewis, M., and D. S. Kessler. 2007. Prevalence of the EH1 Groucho interaction motif in the metazoan Fox family of transcriptional regulators. BMC Genomics. 8:1-17.

Yang, L., Xie, G., Fan, Q., and J. Xie. 2010. Activation of the hedgehog-signaling pathway in human cancer and the clinical implications. Oncogene. 29:469-481.

Yao, T., Ohtani, K., Kuratani, S., and H. Wada. 2011. Development of lamprey mucocartilage and its dorsal-ventral patterning by endothelin signaling, with insight into vertebrate jaw evolution. J Exp Zool B Mol Dev Evol. 316:339-346.

Yen, S., Zhang, M., Deng, J. M., Usman, S. J., Smith, C. N., Parker-Thornburg, J., Swinton, P. G., Martin, J. F., and R. R. Behringer. 2014. Somatic mosaicism and

allele complexity induced by CRISPR/Cas9 RNA injections in mouse zygotes. Dev. Biology. 393:3-9.

Zhang, H., Meng, F., Liu, G., Zhang, B., Zhu, J., Wu, F., Ethier, S. P., Miller, F., and G. Wu. 2011. Forkhead Transcription Factor *Foxq1* Promotes Epithelial-Mesenchymal Transition and Breast Cancer Metastasis. Cancer Res. 71:1292-1301.

Zhang, J., Yang, Y., Yang, T., Yuan, S., Wang, R., Pan, Z., Yang, Y., Huang, G., Gu, F., Jiang, B., Lin, C., and W. Zhou. 2015. Double-Negative Feedback Loop Between MicroRNA-422a and Forkhead Box (FOX)G1/Q1/E1 Regulates Hepatocellular Carcinoma Tumor Growth and Metastasis. Hepatology. 61:561-573.

Zhao, B., and Y. Chen. 2014. Regulation of TGF-β Signal Transduction. Scientifica. 2014:1-9.

Zhu, Z., Zhu, Z., Pang, Z., Xing, Y., Wan, F., Lan, D., and H. Wang. 2013. Short hairpin RNA targeting FOXQ1 inhibits invasion and metastasis via the reversal of epithelial-mesenchymal transition in bladder cancer. International Journal of Oncology. 42:1271-1278.

Zhuang, Y., Faria, T. N., Chambon, P., and L. J. Gudas. 2003. Identification and Characterization of Retinoic Acid Receptor β_2 Target Genes in F9 Teratocarcinoma Cells. Molecular Cancer Research. 1:619-630.